

**JANUARY 2016**

**M.Sc. in Mechanical Engineering**

**IHSAN CIHAN DAI**

**UNIVERSITY OF GAZIANTEP  
GRADUATE SCHOOL OF  
NATURAL & APPLIED SCIENCES**

**STRUCTURAL ANALYSIS AND IMPROVEMENT OF  
FORKLIFT USING FINITE ELEMENT METHOD**

**M.Sc. THESIS  
IN  
MECHANICAL ENGINEERING**

**BY  
IHSAN CIHAN DAI  
JANUARY 2016**

**Structural Analysis and Improvement of Forklift Using  
Finite Element Method**

**M.Sc. Thesis**

**in**

**Mechanical Engineering**

**University of Gaziantep**

**Supervisor**

**Assist. Prof. Dr. Ömer Yavuz BOZKURT**

**By**

**İhsan Cihan DAİ**

**January 2016**

© 2016 [İhsan Cihan DAİ]


REPUBLIC OF TURKEY  
UNIVERSITY OF GAZİANTEP  
GRADUATE SCHOOL OF NATURAL & APPLIED SCIENCES  
MECHANICAL ENGINEERING

Name of the thesis: Structural Analysis and Improvement of Forklift Using Finite Element Method

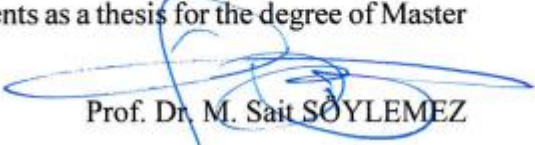
Name of student : İhsan Cihan DAİ

Exam Date : 25.01.2016


Approval of the Graduate School of Natural and Applied Sciences

  
Prof. Dr. Metin BEDİR  
Director

I certify that this thesis satisfies all the requirements as a thesis for the degree of Master of Science.

  
Prof. Dr. M. Sait SÖYLEMEZ  
Head of Department

This is to certify that we have read this thesis and that in our opinion it is fully adequate, in scope and quality, as a thesis for the degree of Master of Science.

  
Assist. Prof. Dr. Ö. Yavuz BOZKURT  
Supervisor

Examining Committee Members

Prof. Dr. Bahattin KANBER

Assoc. Prof. Dr. Ahmet ERKLİĞ

Assoc. Prof. Dr. M. Akif KÜTÜK

Assist. Prof. Dr. Ö. Yavuz BOZKURT

Assist. Prof. Dr. M. Veysel ÇAKIR

Signature

  
.....  
  
.....  
  
.....  
  
.....  
  
.....

**I hereby declare that all information in this document has been obtained and presented in accordance with academic rules and ethical conduct. I also declare that, as required by these rules and conduct, I have cited and referenced all material and results that are not original to this work.**

**İhsan Cihan DAİ**

## **ABSTRACT**

### **STRUCTURAL ANALYSIS AND IMPROVEMENT OF FORKLIFT USING FINITE ELEMENT METHOD**

DAİ, İhsan Cihan

M.Sc. in Mechanical Engineering

Supervisor: Assist. Prof. Dr. Ömer Yavuz BOZKURT

January 2016, 47 pages

In this work, static analysis of structural parts of a diesel forklift were performed using Finite Element Method and possible geometry modifications were utilized with respect to stress distributions at critical regions in order to improve reliability of the forklift design. The analyses were carried out according to standard regulations related with each of the analysed parts. The analysed parts (chassis, head-guard and fork) are the basic building blocks of forklift. The improvements in chases were demonstrated by the comparison of stress values for the original and the modified geometries. It is shown that significant reductions in stress values were obtained without a substantial change in the geometry of the chases. The reliability of head-guard and fork designs were assessed by performing finite element analyses. The finite element analyses were implemented using MSC SimXpert Nastran Finite Element software package.

**Keywords:** Finite element analysis; forklift; MSC SimXpert Nastran

## ÖZET

### SONLU ELEMANLAR METODU KULLANARAK FORKLİFT'İN YAPISAL ANALİZİ VE İYİLEŞTİRİLMESİ

DAİ, İhsan Cihan

Yüksek Lisans Tezi, Makine Mühendisliği Bölümü

Tez Yöneticisi: Yrd. Doç. Dr. Ömer Yavuz BOZKURT

Ocak 2016, 47 sayfa

Bu çalışmada, bir dizel forkliftin yapısal parçalarının statik analizleri Sonlu Elemanlar Metodu kullanılarak yapılmıştır ve forkliftin tasarım güvenilirliğini arttırmak için kritik bölgelerdeki stress dağılımlarına göre geometride değişiklikler yapılmıştır. Analizler, incelenen parçaların her biri ile ilgili standard regülasyonlara göre gerçekleştirilmiştir. Analizi yapılan parçalar (şase, kabin ve çatal) forkliftin temel yapı taşlarını oluşturmaktadır. Şasede yapılan iyileştirmeler orjinal ve değiştirilmiş geometriler için stres değerlerinin karşılaştırılması ile gösterilmiştir. Şase geometrisinde önemli değişiklikler olmadan stres değerlerinde kayda değer azalmalar elde edilmiştir. Kabin ve çatalın tasarım güvenilirliği sonlu elemanlar analizi ile belirlenmiştir. Sonlu elemanlar analizi MSC SimXpert Nastran Sonlu Elemanlar yazılım paketi kullanılarak uygulanmıştır.

**Anahtar Kelimeler:** Sonlu elemanlar analizi; forklift; MSC SimXpert Nastran

*To my wife and family...*



## **ACKNOWLEDGEMENTS**

I want to express my honest respect to my supervisor Assist. Prof. Dr. Ömer Yavuz BOZKURT for his guidance, suggestions and encouragement during master education and preparation of this thesis.

Also, I want to thank my friends for their reassurance and support. Finally, I would like to thank my wife and family for the unwavering moral and emotional support.

## CONTENT

	<b>Page</b>
ABSTRACT .....	v
ÖZET.....	vi
ACKNOWLEDGEMENTS .....	viii
CONTENT .....	ix
LIST OF FIGURES .....	xi
LIST OF TABLES .....	xiii
CHAPTER 1 .....	1
INTRODUCTION .....	1
1.1. General Introduction .....	1
1.2. Research Objectives and Tasks .....	2
1.3. Layout of Thesis.....	2
CHAPTER 2 .....	3
LITERATURE SURVEY .....	3
2.1. Introduction .....	3
2.2. Literature Survey of Finite Element Analysis.....	3
2.3. Conclusion on Literature Survey .....	6
CHAPTER 3 .....	7
FINITE ELEMENT ANALYSIS.....	7
3.1. Introduction .....	7
3.2. Finite Element Method.....	7
3.3. SimXpert Structure Finite Element Analysis Program .....	11
3.3.1. General Information .....	11
3.3.2. Program Capability .....	11
CHAPTER 4 .....	12
ANALYSIS OF FORKLIFT PARTS .....	12
4.1. General View and Technical Parameters .....	12
4.2. Assumptions.....	13
4.3. Analysis of Chassis .....	14
4.3.1. Overload Loading.....	14
4.3.2. Finite Element Analysis of Chassis .....	17
4.3.3. Boundary Conditions of Chassis.....	19

4.3.4. FEA Results of Chassis.....	19
4.3.5. Conclusion on Finite Element Analysis of Chassis .....	21
4.4. Head-guard ROPS Analysis.....	22
4.4.1. Nonlinear Analysis.....	23
4.4.2. ROPS Loadings .....	24
4.4.2.1. Lateral Load and Lateral Load Energy .....	25
4.4.2.2. Vertical Load.....	25
4.4.2.3. Longitudinal Load.....	26
4.4.3. Finite Element Analysis of Head-guard.....	26
4.4.4. Boundary Conditions of Head-guard .....	27
4.4.5. FEM Results of Head-guard .....	28
4.4.5.1. FEM Results of Lateral Loading.....	28
4.4.5.2. FEM Results of Vertical Loading .....	32
4.4.5.3. FEM Results of Longitudinal Loading .....	34
4.4.6. Conclusion on Finite Element Analysis of Head-guard.....	36
4.5. Analysis of Fork.....	37
4.5.1. Finite Element Analysis of Fork .....	38
4.5.2. FEA Results of Fork .....	38
4.5.3. Conclusion on Finite Element Analysis of Fork .....	41
CHAPTER 5 .....	42
CONCLUSIONS.....	42
FUTURE WORKS.....	44
REFERENCES.....	45

## LIST OF FIGURES

	<b>Page</b>
Figure 3.1. Typical finite element mesh. Elements, nodes and edges .....	8
Figure 3.2. Quadrilateral and triangular shell elements .....	10
Figure 3.3. General view of SimXpert structure module .....	11
Figure 4.1. General view of a diesel forklift .....	12
Figure 4.2. The solid model of forklift chassis .....	14
Figure 4.3. Loads acting on chassis. (a) $F_1$ , $F_2$ , $F_3$ , $F_4$ and $F_5$ forces, (b) $F_6$ force ...	15
Figure 4.4. Free body diagram of mast assembly at standard lift height under overload condition.....	17
Figure 4.5. Finite element model of chassis.....	18
Figure 4.6. Stress-Element size curve .....	18
Figure 4.7. The FEA results of chassis. (a) Isometric view of chassis fem result; (b) Side view of chassis fem result; (c) Maximum von Mises stress in tilt cylinder connection bracket.....	20
Figure 4.8. a) The original connection bracket, b) First revision of connection bracket, c) Second revision of connection bracket.....	21
Figure 4.9. 3D solid model of head-guard .....	22
Figure 4.10. 3D solid model of seated operator .....	23
Figure 4.11. Stress-Strain values of material of St 52-3 .....	23
Figure 4.12. Force and energy equations .....	24
Figure 4.13. Finite element model of head-guard .....	26
Figure 4.14. Loading cases of head-guard. (a) $F_{\text{Lateral}}$ force, $FC_1$ , $FC_2$ , $FC_3$ and $FC_4$ fixed constraints; (b) $F_{\text{Vertical}}$ force, $FC_5$ , $FC_6$ , $FC_7$ and $FC_8$ fixed constraints; (c) $F_{\text{Longitudinal}}$ force, $FC_9$ , $FC_{10}$ , $FC_{11}$ and $FC_{12}$ fixed constraints .....	28
Figure 4.15. FEM results of 27000N lateral loading (a)Maximum loading; (b)Load removed.....	29

Figure 4.16. Force-Displacement curve, 27000N loading .....	30
Figure 4.17. The stress results of FEA for the lateral loading with a magnitude of 32000 N (a) When the maximum load is acted; (b) When the load is removed .....	31
Figure 4.18. Force-Displacement curve, 32000N loading .....	32
Figure 4.19. The FEM results of vertical loading on (a) Isometric view; (b) Front view; (c) Side view .....	34
Figure 4.20. FEM results of longitudinal loading (a) Isometric view of fem result; (b) Front view of fem result; (c) Side view of fem result .....	36
Figure 4.21. The solid model of fork .....	37
Figure 4.22. Finite element model of fork with its boundary conditions.....	37
Figure 4.23. Finite element model of fork .....	38
Figure 4.24. The FEA results of fork. (a) Isometric view of fork fem result; (b) Side view of chassis fem result; (c) Isometric view of fork fem result .....	40
Figure 4.25. Displacement result of fork .....	40

## LIST OF TABLES

	<b>Page</b>
Table 4.1. Diesel Forklift Technical Parameters.....	13
Table 4.2. The mechanical properties of St52-3 .....	18
Table 4.3. Comparison of von Mises stresses of tilt cylinder connection bracket.....	21

## CHAPTER 1

### INTRODUCTION

#### 1.1. General Introduction

Forklift is a relatively small industrial vehicle used to carry industrial goods in a short distance by two power-operated forks at the front. It is also called as a lift truck, a fork truck, or a forklift truck. A forklift can be used in numerous places such as; warehouses, factories, farms, shipping yards, construction sites, supermarkets, and much more. Several different forklift models are found in literature. They can be categorized based on their design, i.e. capabilities, size and methods of operation. The capacities of forklifts may range from under 1 tonne to 40 tonnes. Forklifts play a very important role in the life of businesses. To meet needs of business, forklifts have significantly evolved in shape and configuration, such as small forklifts for handling small pallets of goods, large forklifts for moving shipping containers and the use of a whole array of attachments which transform the fork of a forklift into mechanical arms suited to specific goods, such as drums or rolls of carpets or soft cartons and so on.

Forklifts are inherently dangerous vehicles, however, their risk potential cannot be understood at first glance because of their typically compact size. A forklift is a heavyweight vehicle. For example, a counterbalanced forklift with a 2500 kg load capacity, the mass of forklift without and with cargo can be over 3000 kg and 6000 kg, respectively. In the loaded condition, each front wheel has to support nearly 2500 kg load. A useful perspective is that a counterbalanced forklift with a 2500 kg capacity has a weight four times of the average family car weight (1400kg). In addition, the loads are not secured to the vehicle during transportation and this resulted in unstable load configuration coupled with a high momentum vehicle. Due to its heavy working conditions, forklift parts are exposed to high loadings. The parts of a forklift must have a rigid and unyielding construction to support the loads imposed on it. A forklift design must satisfy the requirements of heavy working conditions to prevent failure and to provide long service life.

The tests or testing steps are one of the most important and necessary part of a design procedure. Several tests must be performed to develop a new product. Due to requirement of long time durations and production of a prototype, destructive and non-destructive physical tests are generally expensive and adversely affect the product's time to enter the market. In today's world, computer simulations are carried out to improve the efficiency of design procedures in terms of cost and time by reducing or eliminating the need of physical tests. Finite element method (FEM) is the most widely used numerical analysis method in the computer simulations. The FEM does not require a physical prototype production and it can be used to analyse any parts/components of the whole system under certain operating conditions. Also, it permits improvements in the reliability of product by changing the design according to the results of analysis.

## **1.2. Research Objectives and Tasks**

The main goals of this thesis are the realization of FEA for the chassis, head-guard and fork of a diesel forklift design, and proposition of possible geometry modifications to reduce the stress concentrations in the relevant parts. The stress distributions of main and modified models are compared to ensure reduction in stress concentration. Also, inspection of safety regulations related is an objective of the study.

The research tasks can be shown as follows;

- I. An overview of studies related with the structural analysis of forklifts in the literature.
- II. A short review of the finite element method.
- III. FEA analysis of some structural parts of a forklift.
- IV. Comparison of stress distributions in original and modified geometries of the relevant parts.

## **1.3. Layout of Thesis**

A brief literature survey about the structural analysis of forklifts are provided in chapter two. A short presentation about the FEM and MSC SimXpert are given in chapter three. Static analysis of forklift chassis, head-guard and fork are presented in chapter four. The conclusions are revealed in chapter five.



## CHAPTER 2

### LITERATURE SURVEY

#### 2.1. Introduction

A short review about the structural analysis and design of a forklift and its components using finite element method are presented in the chapter.

#### 2.2. Literature Survey of Finite Element Analysis

The use of forklifts led to rise after the World War II and continued to raise its popularity by providing an imperative role to many industries in their logistic operations. For the last few decades, finite element method has become a vital tool in design and development processes of engineering products (devices, machines, structures, etc.), and has applied in a variety of applications. However, despite popularities of finite element method and forklifts, only a few number of articles associated with the finite element analysis of forklifts have been found in the accessible literature.

Bhagat et al. [1] developed the CAD model of a translation carriage for reach truck and performed the static analyse of it under various loading and boundary conditions using finite element analysis in ANSYS environment. The loading and boundary conditions were determined from the normal and extreme operating conditions. The development of translation carriage for a specified load was carried out according to Indian standards.

Doçi et al. [2] examined the structural behaviours of forklift under dynamic loadings and specified the parameters that affect the dynamic behaviours of forklift. A virtual forklift truck design was prepared and finite element analyses were carried out for the computer simulations. The results of finite element analyses were used to identify the parameters of the forklift design that affect the performance of forklift parts.

Meshram [3] optimized the mast of a forklift to eliminate the problems encountered during lifting a load. For that purpose, 3D models of forklift mast with a small change in geometry are developed. The optimization of forklift mast is performed by conducting the finite element analysis of the forklift mast. In terms of stress distribution, the performance of structural steel and gray cast iron were compared using the same boundary conditions. According to the result of FEA, the structural steel is suggested for the mast of forklift.

Rane et al. [4] carried out topology optimization technique for the design of forklift chassis to reduce the weight without changing the working conditions of forklift. The analyses were carried out using different boundary conditions, and the changes in stress and weight were compared to investigate performance of optimization. A significant weight reduction without a remarkable change in deflection was reported as result of the study.

Cline [5] seeked the failure of forks of an over-sized forklift during the transportation of ship container. The fracture due to fatigue was detected as the source of the failure. The finite element analyses of fork was carried out using centred and moderately offset load configurations. The fatigue life of the forks were estimated and the number of load cycles for fatigue failure was evaluated from the estimated fatigue life.

Miralbes et al. [6] proposed a new methodology to optimize the mechanical design of the crane gibs and pallet box lock for a forklift truck. The finite element method was used as a numerical tool for proposed method and the boundary conditions were provided according to the forklift truck regulations. The reliability of the proposed method was verified using the experimental results.

Stoychev and Chankov [7] proposed a dynamic model to investigate the stresses for the lifting installation of a forklift truck. The elasticity and damping characteristics of the tilt cylinder has been identified by conducting finite element analysis. The finite element analyses were performed using the COSMOS/M traditional software package. The validity of finite element analysis was checked by comparison with experimental results.

Todorov et al. [8] presented a demonstration of contemporary approach for product design development. A virtual design of a forklift transmission module for an electric forklift was developed for the investigation of design parameters. Thermal and structural analysis were carried using finite element method to improve the design and to obtain a competitive product with a less cost.

Slavchev [9] studied the stressed state problems at folded region of fork arms for forklifts with different load carrying capacities and different modes of attachment to the carrying plate. The forklift arms were modelled in computer environment for the stress analyses. The analyses were carried out by the employment of FEM to 3D computer models of forklift arms. The results of the analyses were verified by corresponding strain-gauging measurements.

Yao et al. [10] proposed a new kind of lifting mechanism for hybrid forklift truck. The 3D models of lifting mechanism was constructed in CATIA 3D software and used in ANSYS software for the finite element analyse. By considering maximum deformation extent and deformation stress points, the performance of lifting mechanism had been investigated under different working conditions such as upright mounting load, upright mounting rise, upright mounting decline and maximum deformation extent. According to the results of analyses, new lifting mechanism satisfied the design requirements.

Sachin et al. [11] prepared a fork design for the forklift truck and performed the finite element analysis of fork. The 3D model of fork prototype was prepared in Pro-E 5.0 solid modeling software and the finite element analyses were carried out using ANSYS software. The results of the finite element analysis and theoretical calculations were compared to validate the finite element analysis. Due to its advantages, mild steel was preferred in the selection of material.

Zeng et al. [12] worked on the optimization of the forklift truck frame system. The virtual prototype model of forklift truck system was generated by forwarding the 3D model of fork truck frame created in Pro/E software program into the ADAMS dynamic simulation software. The finite element analysis was performed on ANSYS using the boundary conditions taken from dynamic analysis such as load and displacement.

Figueiredo et al. [13] investigated the fracture of two forks of a heavy duty lift truck by conducting a series of failure analysis. The study of failure analyses include characterization of the material, examination of the previous welding repair in one of the forks, detection of the weld defects, identification of fatigue cracks and stress analysis using finite element method. A systematic methodology was provided for the failure analysis.

Erkliđ et al. [14] has carried out the finite element analysis of backhoe loader arms. As a result of analysis at maximum and different operating conditions, stresses in the critical points were identified. As a result of improvements in geometry, critical stresses were reduced.

### **2.3. Conclusion on Literature Survey**

The following conclusions were obtained from the literature reviews;

- Several studies were dealt with the design and analyses of separate parts of forklift.
- A few studies interest with the design of separate parts using optimization techniques such as topology optimization.
- Some studies examined the structural behaviours of forklift parts under dynamic loads.

To author's knowledge, have no open literature available on the ROPS (Roll-Over Protective Structures) analysis of head-guard and the finite element analyses of chassis, head-guard and fork at the same study. With respect to literature review, the main subject of this thesis is the finite element analysis of chassis, head-guard and fork.

The specific goals are;

- Improvement of the reliability of forklift chassis by conducting finite element analysis.
- Execution of finite element method for the ROPS analyses of head-guard and examination of the reliability of head-guard design
- Finite element analysis of fork under overload at standard load distance.

## CHAPTER 3

### FINITE ELEMENT ANALYSIS

#### 3.1 Introduction

Some basic information about finite element method and a short description of MSC SimXpert software program is presented in the following sections of this chapter.

#### 3.2 Finite Element Method

Finite element is one of the most widely used numerical methods for finding solutions to boundary value problems that arise in different applications of science and engineering such as solid mechanics [17], fluid mechanics [18], acoustic [19], electromagnetism [20] and heat transfer [21]. Because of the difficulties involved in obtaining exact closed-form solutions, finite element method has been often employed to find approximate solutions to the complex industrial problems.

The finite element method is discussed for the first time in 1940s by Richard Courant and Alexander Hrennikoff [22]. In the 1950s it began to be used in the aircraft industry. "Finite element" statement is used in the article for the first time in 1960 by Ray William Clough [23]. John Argyris, with studies in the 1960s and 1970s, has accelerated the development of finite element method. In the late 1980s, finite element analysis software programs started to be used at computers. Among the various numerical methods, the finite difference, finite volume, boundary element and finite element method, the most evolved and the most commonly one is the finite element method. Over the past 20 years, the use of finite element method shows a rapid increase parallel to the development of computer hardware, and because of its diversity and flexibility it also receives significant attentions in engineering education and in industry as an analysis tool.

The entire problem domain is divided into smaller subdomains in the form of a definite geometry that surrounded with certain points. The elements are connected to

each other at common nodes. The subdomains and points are called as elements and nodes, respectively. Instead of solving the problem for the whole domain, solution of the problem is carried out within each element and then the solution information of each element is joined together to form a solution for the whole problem domain. The solution in an element is based on approximation and formulation of system equations. The approximation in an element is performed using shape functions. The combination of nodes and elements are called as “finite element mesh” or simply “mesh”. Mesh is programmed with material properties to determine the behaviour of problem structure under certain boundary conditions.

The solution procedure of the finite element method for a problem related to solid body mechanics is performed by the following step by step process;

1. Discretization

Problem domain are divided into non-overlapping sub-regions or elements. Several types of element shapes, such as triangles, quadrilaterals can be found in finite element discretization. Elements can also show variations according to number of nodes used in the interpolation of field variables. Each element is defined using the information of nodal connectivity's as shown in Fig. 3.1.

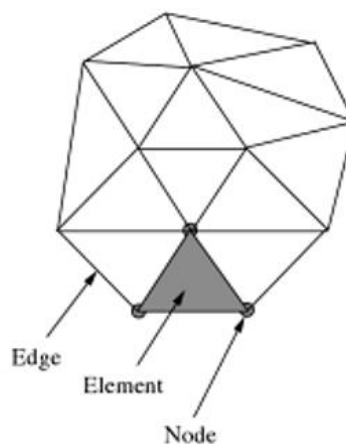


**Figure 3.1.** Typical finite element mesh. Elements, nodes and edges

2. Choosing of interpolation or shape functions

Second step is the representation of the field variable variation over an element by means of interpolation function. The variation of a field variable within the

element is characterized by the number of nodes on the element and number of unknowns at each node.

### 3. Formulation of element equations

After the second step, the individual element properties and the loads applied on are expressed as stiffness matrix and load vector of the element, respectively. For example, stiffness matrix and load vector for a typical quadrilateral element can be written as

$$[\mathbf{K}]_e = \int_{-1}^{+1} \int_{-1}^{+1} \mathbf{B}^T \mathbf{D} \mathbf{B} \det(\mathbf{Jac}) d\xi d\eta \quad (3.1)$$

$$\{\mathbf{f}\}_e = [f_{1x} \ f_{1y} \ f_{2x} \ f_{2y} \ f_{3x} \ f_{3y} \ f_{4x} \ f_{4y}] \quad (3.2)$$

where  $\mathbf{B}$  is the matrix that contains the derivatives of shape functions,  $\mathbf{D}$  is the material matrix,  $\mathbf{Jac}$  is the Jacobian matrix and  $\mathbf{f}$  is the force applied to the nodes of element. The subscript “e” represents an element, the subscripts “1,2,3,4” denotes the local node numbers of the element, and subscript  $x$  and  $y$  represents the direction of forces.

### 4. Assemble of the element equations

To obtain a system of simultaneous equations, assemble of the element equations are performed that means the combining of the matrix equations for each element in a suitable way. For example, the assembly matrix gives the behaviour of whole solution of the problem domain. After the assemblage of the individual element contributions, the boundary conditions must be joined, that is,

$$[\mathbf{K}]\{\mathbf{u}\} = \{\mathbf{f}\} \quad (3.3)$$

where  $[\mathbf{K}]$  is the global stiffness matrix obtained from the assembly of the stiffness matrices of individual elements, as given in Eq. 3.1,  $\{\mathbf{f}\}$  is the global the assembly of load vectors of individual elements, as given in Eq. 3.2, and  $\{\mathbf{u}\}$  is the global unknown vector.

### 5. Solution of the system equations

In this step, resulted system equations in Eq. 3.3 are solved according to obtained the nodal values of the field variables such as displacement.

### 6. Calculate the secondary quantities

This step is related to secondary quantities for the nodal values of field variables like stress that calculated after the solution of the system equations.

The advantages of the finite element method are;

- allow the examination of complex shapes of geometries
- apply different designs and materials
- solve many problems for the same model
- optimize designs
- reduce physical prototyping and testing
- improve product performance and reliability
- use for engineering applications with many softwares such as NASTRAN, MARC, PATRAN, ANSYS, ABAQUS etc.

Also the disadvantages of finite element method are;

- the difficulties at implementation of problems with complex geometries, crack propagation problems and explosion problems,
- mesh quality dependent accuracy for the results,
- the requirement of error controls for modelling errors prior to use of results.

Finite element models can be generated using one-dimensional elements such as beam, two-dimensional elements such as plane, plate and shell elements or three-dimensional solid elements. Examples of 2D shell elements as quadrilateral and triangular are shown below.

1600 | CQUAD4  
Quadrilateral Plate Element Connection

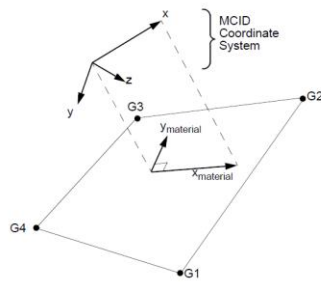


Figure 8-52 MCID Coordinate System Definition

CTRIA3 | 1667  
Triangular Plate Element Connection

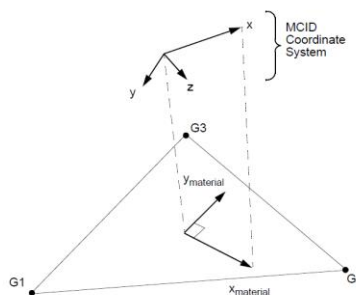


Figure 8-74 MCID Coordinate System Definition

**Figure 3.2.** Quadrilateral and triangular shell elements.



### 3.3 SimXpert Structure Finite Element Analysis Program

#### 3.3.1 General Information

SimXpert is a general purpose computer aided engineering software for finite element analysis. It facilitates manufacturers to accelerate the speed and accuracy of simulation, increase design productivity, and bring better products to market faster. SimXpert includes a series of modules to perform structural, dynamic and thermal analysis.

#### 3.3.2 Program Capability

SimXpert Structure module, an interface for Nastran solver, is a structural analysis software. SimXpert Structure module can handle comprehensive linear and nonlinear finite element analysis. The main features of SimXpert are provided in its workspace. The generation of CAD model of parts to be analysed is the starting point of pre-processor of the SimXpert. Generally, the solid models are imported from any solid modelling software to the SimXpert workspace in stp, parasolid, or other formats. A mesh structure is generated for the CAD model of parts by dividing the geometries of parts into elements. After the mesh generation, the material properties of each element related with each part are separately provided in the pre-processor step of analysis. The boundary conditions in terms of displacement and load are defined according to the type of problem. After the solution, the results of analysis are examined. General view of SimXpert Structure module is given in the Fig. 3.3.

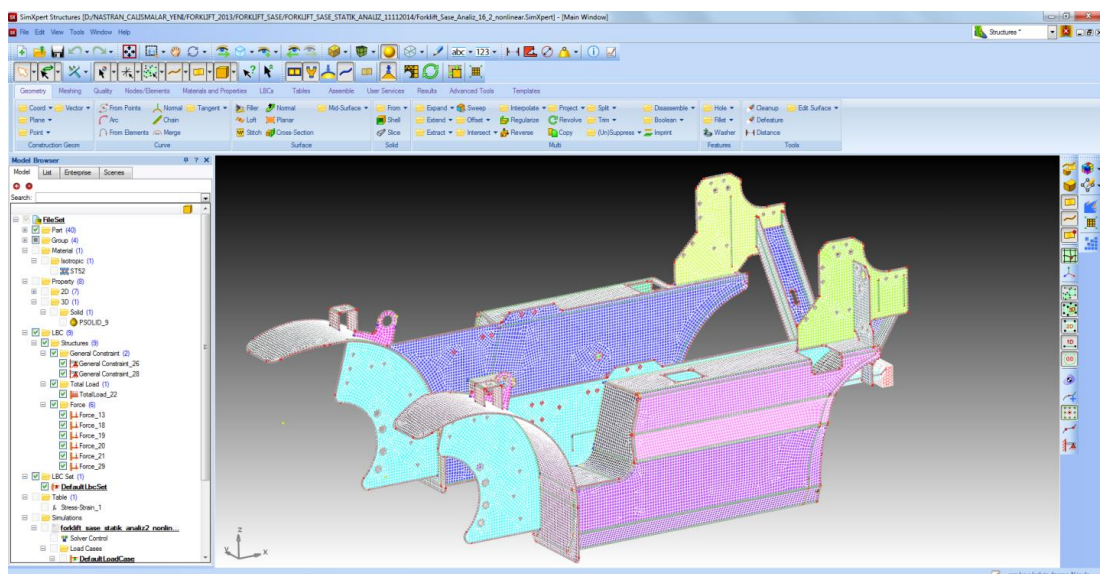


Figure 3.3. General view of SimXpert structure module.

## CHAPTER 4

### ANALYSIS OF FORKLIFT PARTS

#### 4.1 General View and Technical Parameters

General view of the diesel forklift marked with major parts is shown in Fig. 4.1 and some of its technical specifications such as carrying capacity, dimensions, engine power and driving speed are presented in Table 4.1.

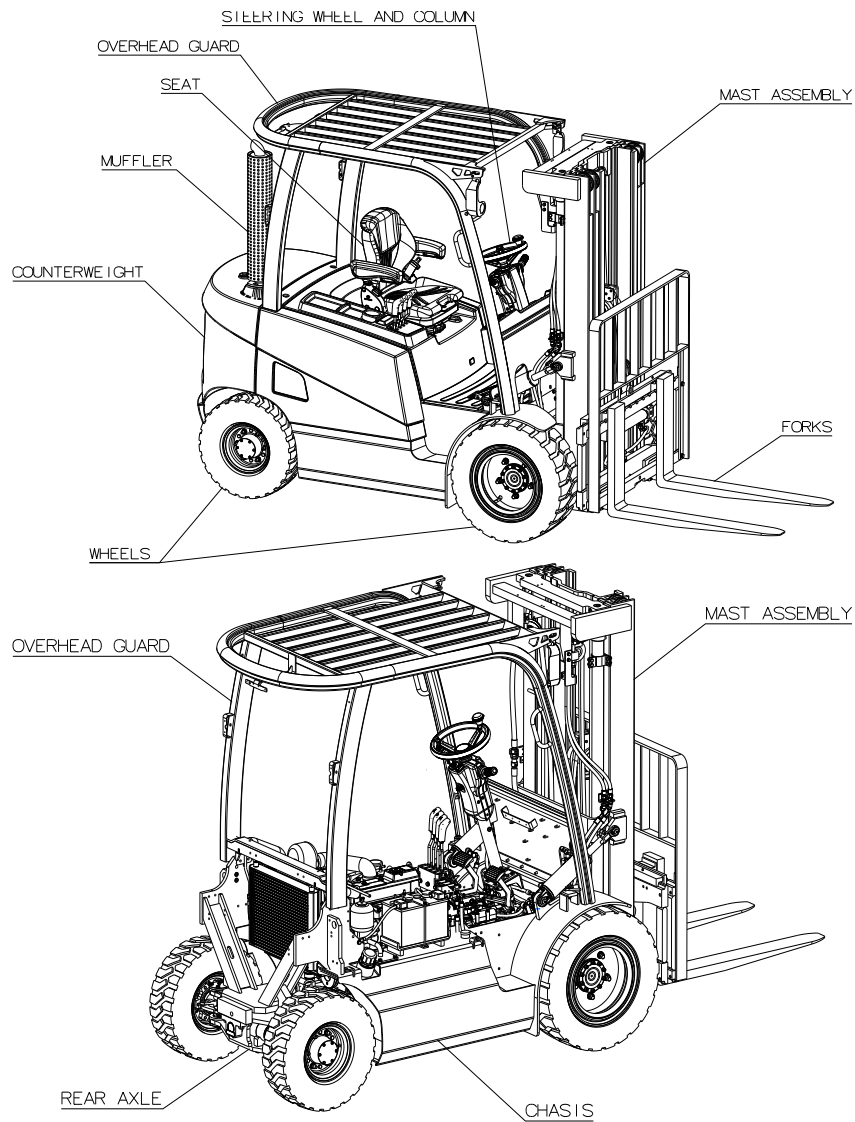


**Figure 4.1.** General view of a diesel forklift.

**Table 4.1.** Diesel Forklift Technical Parameters.

Power unit	Diesel
Carrying capacity/load	3000 kg
Load center	500 mm
Wheel base	1720 mm
Weight	4500 kg
Tilt angle, mast/fork carriage forwards	6°
Tilt angle, mast/fork carriage backwards	10°
Lift height	3230 mm
Overall length	3757 mm
Fork thickness	45 mm
Fork width	100 mm
Fork length	1000 mm
Fork carriage DIN 15173	2A
Turning radius	2400 mm
Driving speed with load	18.2 km/h
Driving speed without load	19.5 km/h
Engine Power	35,5 kW @ 2400 rpm

## 4.2 Assumptions

The finite element analysis of chassis, head-guard and fork were carried out using the following assumptions;

- deformations and strains are small,
- material is linear elastic,
- loads are statically applied to the analyzed parts,
- surfaces are combined in the places of welded joints,
- no changing occurs at material properties after the welding operation.

### 4.3 Analysis of Chassis

The chassis to which all other components are attached is the backbone or the main supporting structure of the forklift truck. The 3D solid model of the chassis of forklift truck, shown in Fig. 4.2, is developed using CATIA 3D solid modelling software. The chassis was fabricated by the weldment of several metal plates. The thickness of plates were range from 6 mm to 40 mm. The chassis is subjected to the forces of tilt cylinders, total weight of cabin with seat, bonnet and operator, total weight of engine with transmission, weight of radiator, total weight of rear axle with wheels, total weight of counterweight and muffler. The calculations of these loads are carried out using static loading, rigid connection member and linear-elastic material behaviour assumptions.

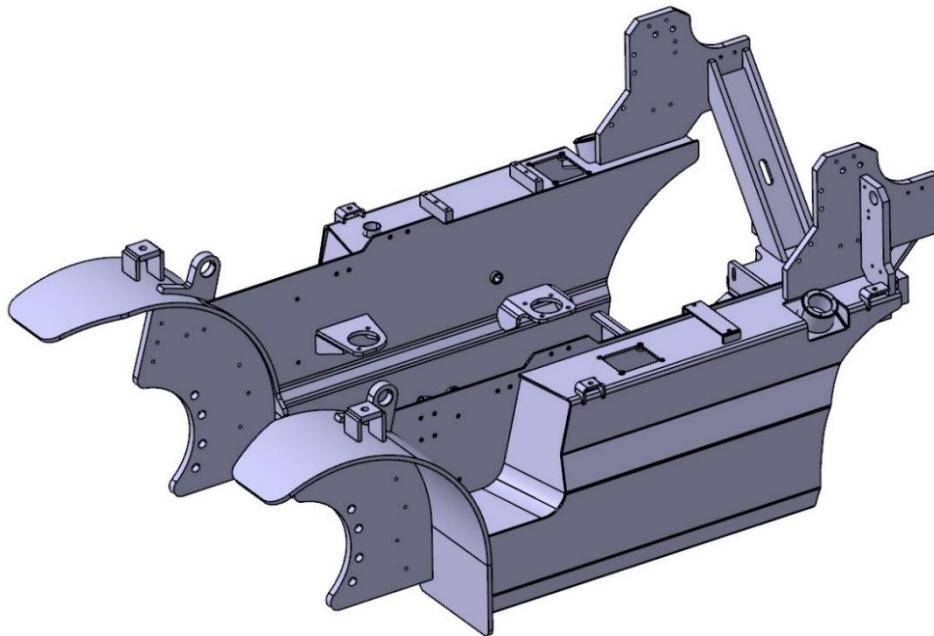
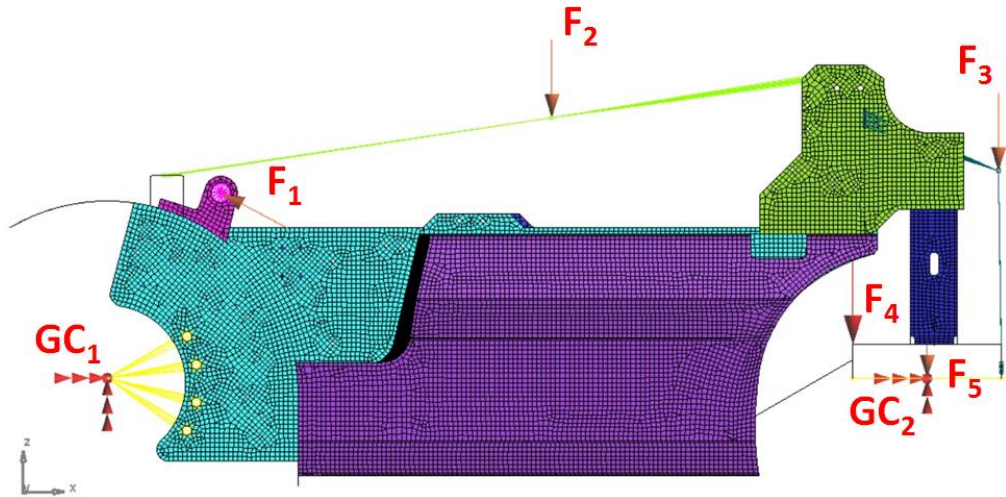


**Figure 4.2.**The solid model of forklift chassis.

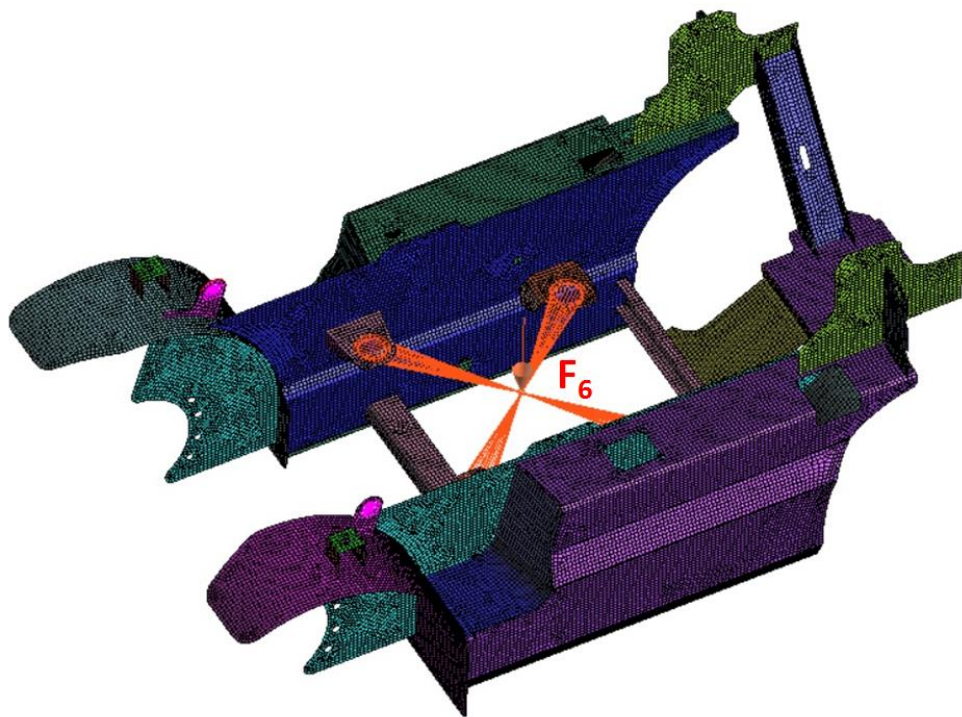
#### 4.3.1 Overload Loading

The load carrying capacity is considered as the first performance characteristics of a forklift truck. The intended maximum load carrying capacity of the analyzed forklift truck is 3000 kg. According to the EN ISO 3691 – 1:2012 standard [15], the structural components of the truck and its attachments shall carry the static load of  $1.33 \times 3000$  kg. It is the rated capacity at standard lift height and standard load center distance with respect to the information on the capacity plate.

The various loads acting on the chassis are shown in Fig. 4.3. The forces of tilt cylinders ( $F_1$ ), total weight of cabin with seat, bonnet and operator ( $F_2$ ), total weight of counterweight and muffler ( $F_3$ ), weight of radiator ( $F_4$ ), total weight of rear axle with wheels ( $F_5$ ), and total weight of engine with transmission ( $F_6$ ) are calculated as 97889.79 N, 2943 N, 17461.8 N, 294.3 N, 1589.2 N and 7700.8 N, respectively.



(a)



(b)

**Figure 4.3.** Loads acting on chassis. (a)  $F_1$ ,  $F_2$ ,  $F_3$ ,  $F_4$  and  $F_5$  forces, (b)  $F_6$  force.

The forces of tilt cylinders were examined using loading process of mast assembly at standard lift height under overload condition. The free body diagram of mast assembly is shown on Fig. 4.4. The mass of mast assembly is 1000 kg. The  $W_1$  and  $W_2$  are the weights of pay load and mast assembly, respectively, and are calculated as  $W_1 = 39141.9$  N,  $W_2 = 9810$  N.

The forces acting to the chassis from the connection point of the tilt cylinders are calculated based on the moment of the axle center of rotation, as follows:

$$\sum M = 0 \quad (4.1)$$

$$W_1 \times 1080 + W_2 \times 379 + F_{1Z} \times 233 - F_{1X} \times 656 = 0 \quad (4.2)$$

where

$$F_{1Z} = F_1 \times \sin 28^\circ \quad (4.3)$$

and

$$F_{1X} = F_1 \times \cos 28^\circ \quad (4.4)$$

The force  $F_1$  and its components  $F_{1Z}$  and  $F_{1X}$  are found as 97889.79 N, 45956.47 N and 86431.55 N, respectively.

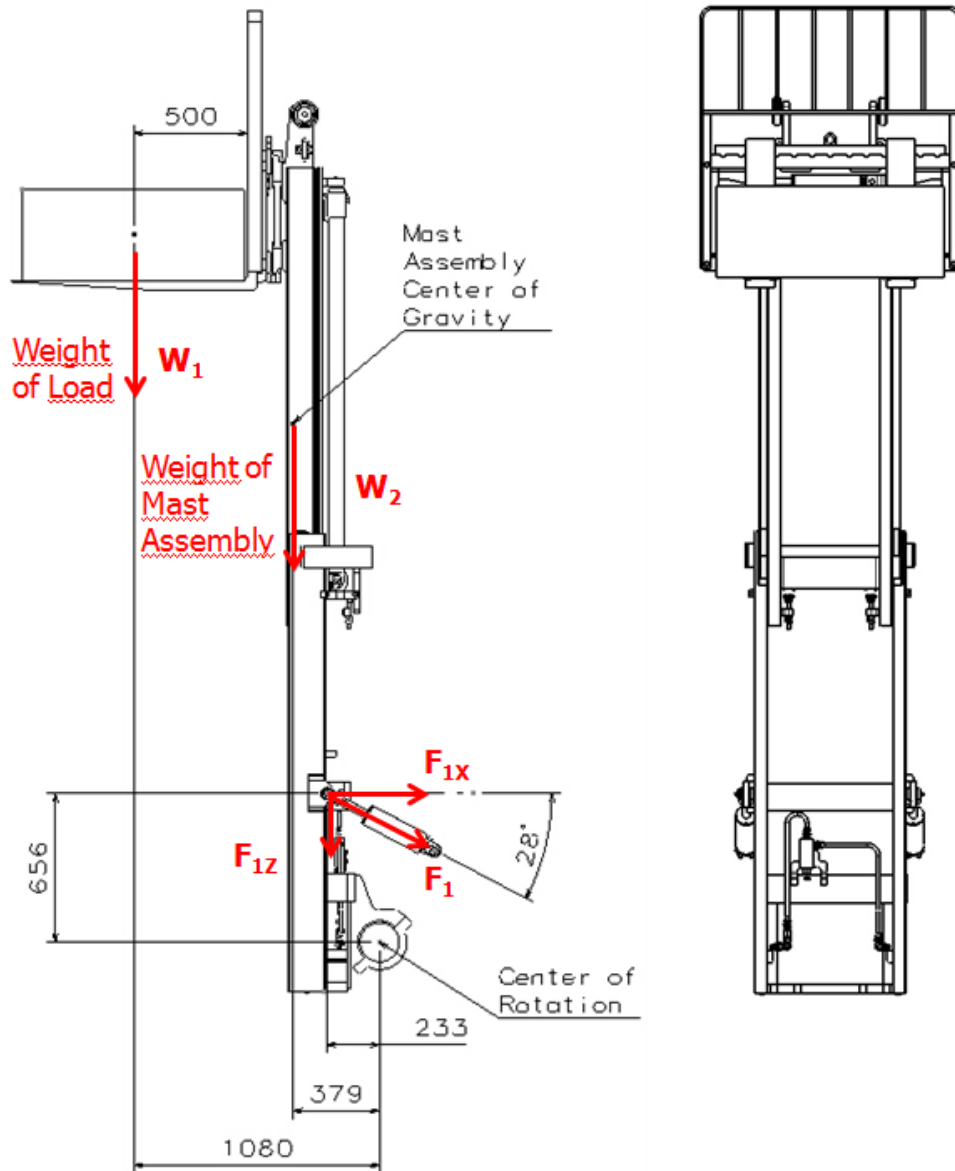


**Figure 4.4.** Free body diagram of mast assembly at standard lift height under overload condition.

### 4.3.2 Finite Element Analysis of Chassis

The finite element model of chassis, shown in Fig. 4.2, is generated using 57293 shell elements with 57473 nodes in SimXpert Structure Analysis program. The elements type used in the model are CQUAD4 and CTRIA3. The finite element model of chassis is shown in Fig. 4.5. The chassis is made of St52-3 and the mechanical properties of St52-3 are given in Table 4.2. The element size is selected as 10 mm according to the element size vs stress assessment shown in Fig. 4.6.

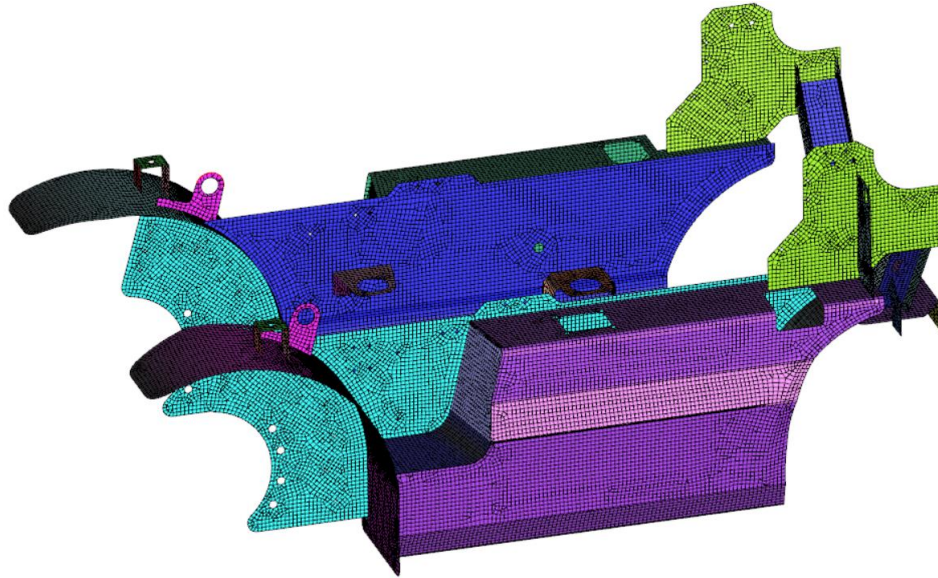


**Figure 4.5.** Finite element model of chassis.

**Table 4.2.** The mechanical properties of St52-3.

Material	St 52-3
Yield Stress (MPa)	355
Ultimate Stress (MPa)	530
Poisson's Ratio	0.3
Young's Modulus (GPa)	210

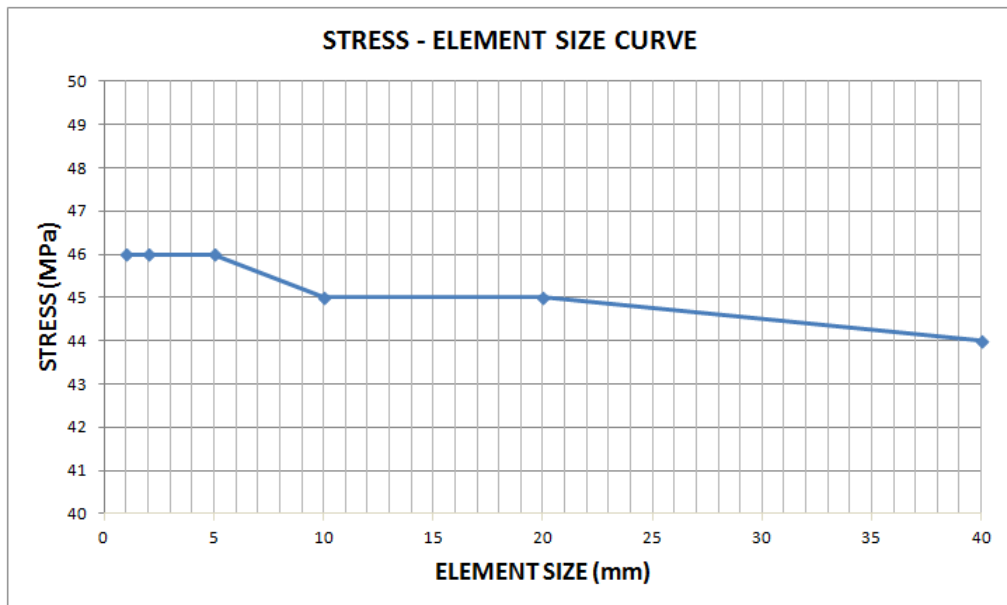


**Figure 4.6.** Stress-Element size curve

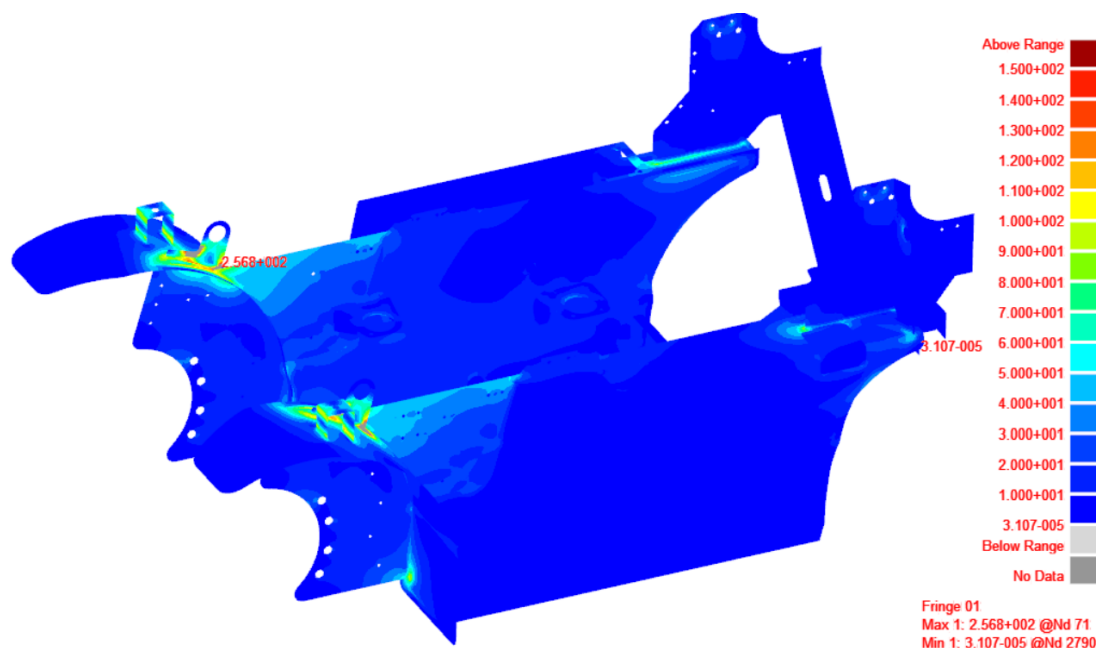


### 4.3.3 Boundary Conditions of Chassis

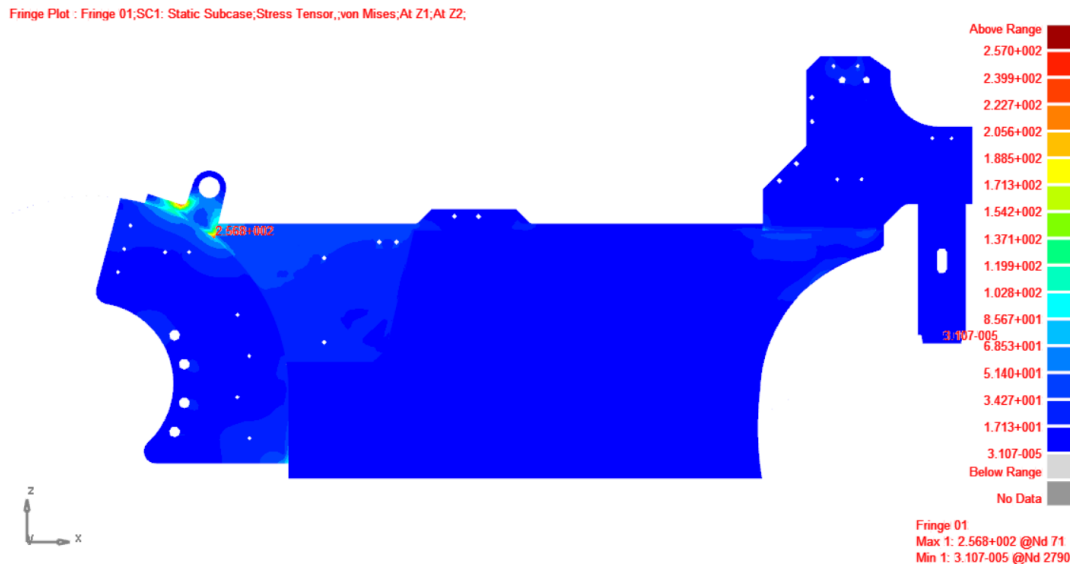
Lifting too much weight can raise the rear wheels and the boundary conditions GC1 and GC2, shown in Fig. 4.3a, are defined by considering this possibility. GC1 shows the rotation of chassis according to axle center of front wheels. All degrees of freedom except the rotation about  $y$ -axis is restrained. GC2 includes three rotational constraints (angular along the  $x$ -,  $y$ -, and  $z$ -axis) and two translational constraints (linear along the  $x$ - and  $y$ -axis).

### 4.3.4 FEA Results of Chassis

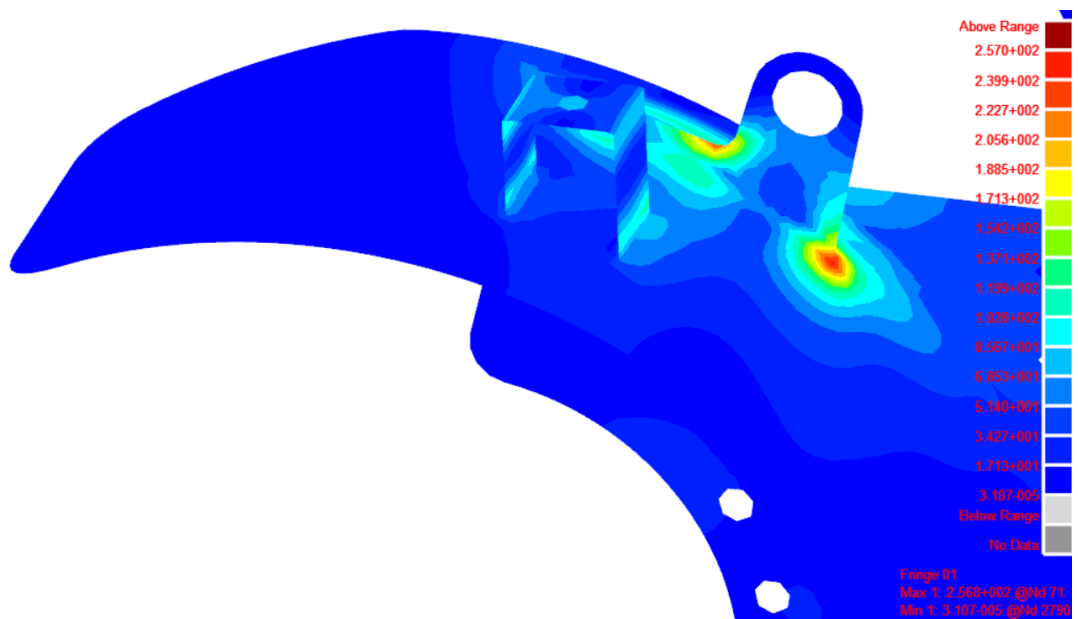
The analysis of chassis is carried out in case of overload at standard lifting height, and the results are shown in Fig. 4.7. It is shown that the maximum von Mises stress is calculated as 257 MPa at the connection bracket of tilt cylinders. The resulting stress is below the yield stress value of St52-3 material. So, there is no plastic deformation on this bracket. However, a stress concentration is shown and a design revision in geometry of bracket should be required to reduce stress values.



(a)



(b)



(c)

**Figure 4.7.** The FEA results of chassis. (a) Isometric view of chassis fem result; (b) Side view of chassis fem result; (c) Maximum von Mises stress in tilt cylinder connection bracket.

The front and rear tips of connection bracket show 232 MPa and 257 MPa for the magnitude of von Mises stress. The front and rear tip points are marked as A and B, respectively. Two new geometries are designed to improve reliability of connection bracket by reducing stress values. Finite element analysis of chassis has been

performed for the new connection bracket designs and the results in terms of von Mises stress distribution are shown in Fig. 4.8. The first design revision in geometry made possible to reduce maximum von Mises stress to 214 MPa from 257 MPa and second one reduced to 136 MPa. The von Mises stress comparisons of original and revised geometries of connection bracket is given in Table 4.3. As seen in Table 4.3, the factor of safety with respect to connection bracket design was increased from 1.38 to 2.08.

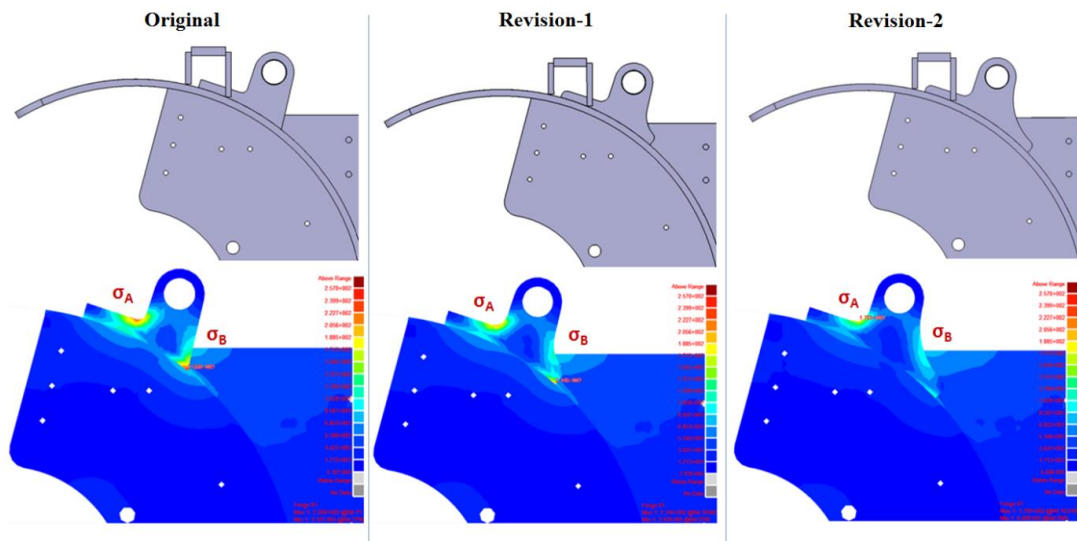


**Figure 4.8.** a) The original connection bracket, b) First revision of connection bracket, c) Second revision of connection bracket.

**Table 4.3.** Comparison of von Mises stresses of tilt cylinder connection bracket.

Von Mises Stress	Original Geometry	Revision-1	Revision-2
$\sigma_A$ (MPa)	232	206	171
$\sigma_B$ (MPa)	257	214	136
Factor of Safety	1.38	1.66	2.08

#### 4.3.5 Conclusion on Finite Element Analysis of Chassis

In this section, static analysis of chassis was carried out. With respect to EN ISO 3691 – 1:2012 standard [15], the static load of  $1.33 \times 3000$  kg is applied to standard load distance on fork at standard lift height. Stress concentration at the connection bracket of tilt cylinder was established. The maximum von Mises stress and the factor of safety were evaluated as 257 MPa and 1.38, respectively. To

alleviate the stress concentration, basic geometry changes were applied to connection bracket. The stress reductions were provided with the geometry changes. For the geometry “revision-2”, the maximum von Mises stress have been reduced to 171 MPa with the provided improvements in geometry. At the same time, the safety factor is increased to 2.08. The reliability of chassis was improved with these basic geometry modifications. It can be concluded that the reliability of chassis can be further improved with any extra geometrical modifications.

#### 4.4 Head-guard ROPS Analysis

Head-guard is an important part of the forklift truck in terms of operator safety. The construction machineries have to satisfy with certain standards/regulations for operator safety. Over head-guard must be designed in accordance with ROPS standard against to overturn to avoid any damage to the operator. In this section, ROPS (Roll-over protective structures) analyses of the forklift truck with its protective structure is carried out in accordance with EN ISO 3471:2008 [16]. The solid model of head-guard, prepared using CATIA 3D solid modelling software, is given in the Fig. 4.9. The seated operator is used in the analysis as described in the EN ISO 3411 standard. The solid model of the seated operator is shown on the Fig. 4.10. In the analysis, seated operator is positioned to the sip point. At the end of the loading procedure, head-guard must not enter the seated operator area.

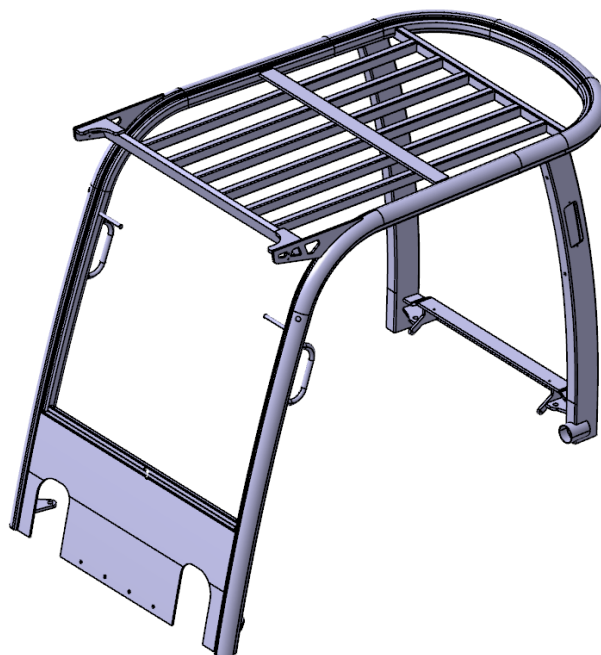


**Figure 4.9.** 3D solid model of head-guard.

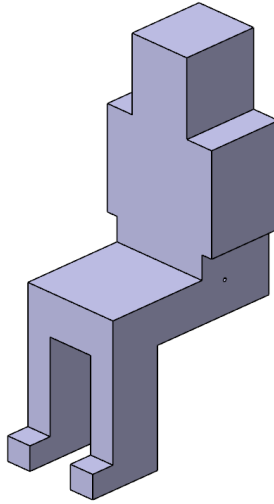


**Figure 4.10.** 3D solid model of seated operator.

#### 4.4.1 Nonlinear Analysis

In the analysis of ROPS, material of the head-guard is recognized as St 52-3. The technical properties of material of St 52-3 are given in the Table 4.2. In the ROPS analysis, stress values can be over the yield stress value. That's why, the ROPS analysis of head-guard was performed as nonlinear analysis. The stress-strain values of material of St 52-3, shown in the Fig. 4.11, are defined in SimXpert software program. Nastran Solver, SOL400 General Nonlinear Analysis, is used as solution type.

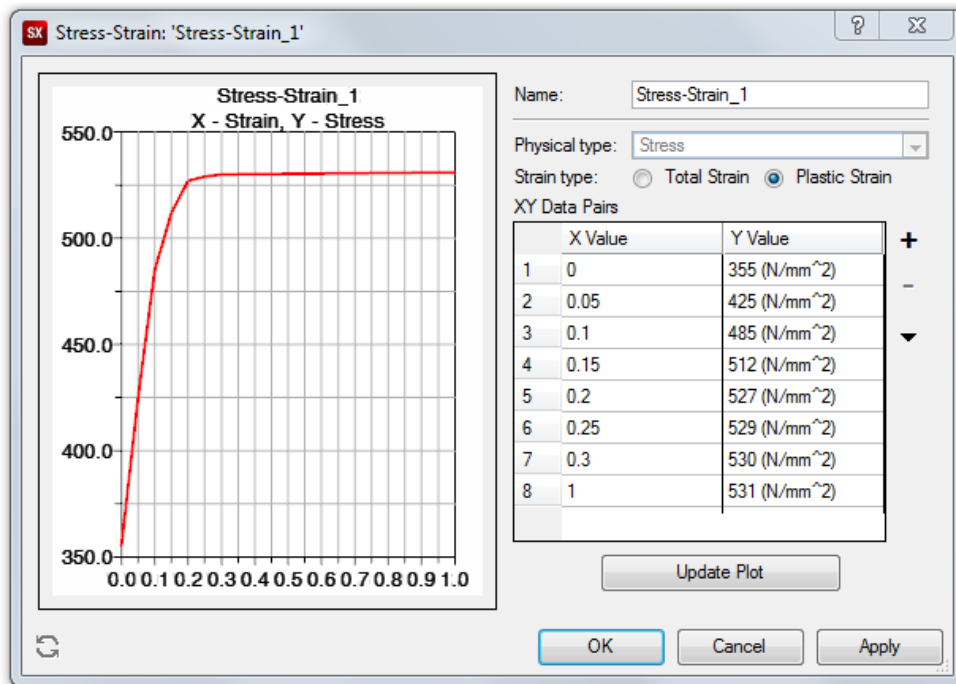


**Figure 4.11.** Stress-Strain values of material of St 52-3.

#### 4.4.2 ROPS Loadings

The loadings of ROPS analysis are determined according to EN ISO 3471:2008 ROPS standard [16]. The magnitudes of loads with respect to the weight of the forklift truck. The weight of forklift truck  $M$  is given in the Table 4.1. The forces are effected in the lateral, vertical and longitudinal directions, and the amount of absorbed energy in the lateral direction must met at least the specified value in EN ISO 3471:2008 ROPS standard [16]. According to the ROPS standard, forklift truck is classified in the wheeled earth-moving machine category.

The equations of lateral load force, lateral load energy (strain energy due to lateral load), vertical load force and longitudinal load force were determined according to EN ISO 3471:2008 ROPS standard [16]. The equations were selected according to the following conditions and chart (shown in Fig. 4.12) of EN ISO 3471:2008 ROPS standard [16].

$$700 < M \leq 10\,000 \quad (4.5)$$

Machine mass $m$ kg	Lateral load force $F$ N	Lateral load energy $U$ J	Vertical load force $F$ N	Longitudinal load force $F$ N
<b>1) Crawler earth-moving machine: dozer, loader, pipelayer and trencher type</b>				
$700 < m \leq 4\,630$	$6m$	$13\,000 (m/10\,000)^{1.25}$	$19,61m$	$4,8m$
$4\,630 < m \leq 59\,500$	$70\,000 (m/10\,000)^{1.2}$	$13\,000 (m/10\,000)^{1.25}$		$56\,000 (m/10\,000)^{1.2}$
$m > 59\,500$	$10m$	$2,03m$		$8m$
<b>2) Grader</b>				
$700 < m \leq 2\,140$	$6m$	$15\,000 (m/10\,000)^{1.25}$	$19,61m$	$4,8m$
$2\,140 < m \leq 38\,010$	$70\,000 (m/10\,000)^{1.1}$	$15\,000 (m/10\,000)^{1.25}$		$56\,000 (m/10\,000)^{1.1}$
$m > 38\,010$	$8m$	$2,09m$		$6,4m$
<b>3) Wheeled earth-moving machine: loader, tractor-dozer, pipelayer, landfill compactor, skid-steer loader, backhoe loader and trencher type</b>				
$700 < m \leq 10\,000$	$6m$	$12\,500 (m/10\,000)^{1.25}$	$19,61m$	$4,8m$
$10\,000 < m \leq 128\,600$	$60\,000 (m/10\,000)^{1.2}$	$12\,500 (m/10\,000)^{1.25}$		$48\,000 (m/10\,000)^{1.2}$
$m > 128\,600$	$10m$	$2,37m$		$8m$
<b>4) Tractor section of combined earth-moving machine: tractor scraper, articulated frame dumper</b>				

Figure 4.12. Force and energy equations.

#### 4.4.2.1 Lateral Load and Lateral Load Energy

The magnitude of lateral load is calculated as below:

$$\begin{aligned} F_{Lateral} &= 6 \times M \\ &= 6 \times 4500 \\ &= 27000 \text{ N} \end{aligned} \quad (4.6)$$

The amount of lateral load energy is specified as below:

$$\begin{aligned} E_{Lateral} &= 12500 \times (M \div 10000)^{1,25} \\ &= 12500 \times (4500 \div 10000)^{1,25} \\ &= 4607 \text{ J} \end{aligned} \quad (4.7)$$

#### 4.4.2.2 Vertical Load

The magnitude of vertical load is calculated as below:

$$\begin{aligned} F_{Vertical} &= 19.6 \times M \\ &= 19.6 \times 4500 \\ &= 88200 \text{ N} \end{aligned} \quad (4.8)$$

The critical buckling load,  $P_{cr}$  must be determined to provide reliable analysis of head-guard having 1.358 m length,  $L$  column and is found by using following formula,

$$P_{cr} = n \frac{\pi^2 EI}{L_e^2} = 8150000 \text{ N} \quad (4.9)$$

where  $n = 2$  and  $L_e = 0.5 * L$  are the constant coefficient and the effective length of the column for the fixed end-fixed end condition,  $E$  is the Young's modulus of the St52-3 is given in Table 2 and  $I$  is the inertia of the material having hollow cross section is calculated below:

$$I = \frac{\pi}{4} (r_o^4 - r_i^4) = 453.25 * 10^{-9} \text{ m}^4 \quad (4.10)$$

where  $r_o$  and  $r_i$  equal to 70 mm and 62 mm, respectively.

It is shown that buckling has not been observed under the vertical loading condition.

#### 4.4.2.3 Longitudinal Load

The magnitude of longitudinal load is calculated as below:

$$\begin{aligned} F_{Longitudinal} &= 4.8 \times M \\ &= 4.8 \times 4500 \\ &= 21600 \text{ N} \end{aligned} \tag{4.11}$$

#### 4.4.3 Finite Element Analysis of Head-guard

The finite element model of head-guard, shown in Fig. 4.13, is generated using 23309 shell elements with 23305 nodes. The elements type used in the model are CQUAD4 and CTRIA3. The load distribution devices used in the head-guard is meshed with solid elements. The head-guard is made of St52-3 and the mechanical properties of St52-3 are given in Table 4.2.

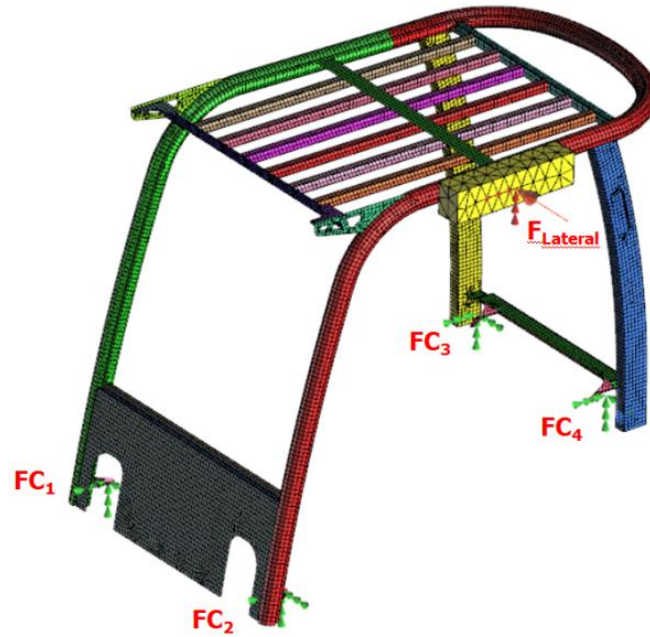


**Figure 4.13.** Finite element model of head-guard.

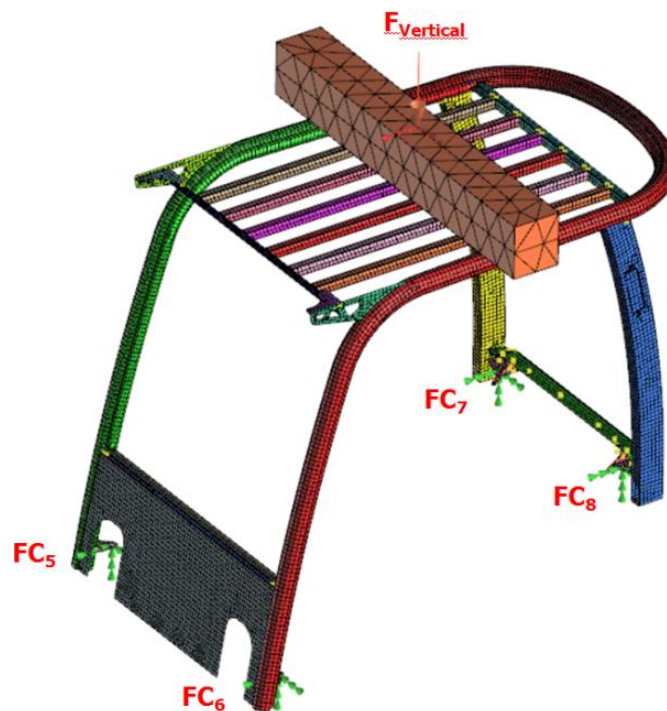


#### 4.4.4 Boundary Conditions of Head-guard

The forces acting on the head-guard are shown on the Fig. 4.14. Load distribution devices for all loading procedure are also shown on the Fig. 4.14.  $F_{Lateral}$  force was calculated as 27000 N using Eq. 4.6,  $F_{Vertical}$  force was calculated as 88200 N using Eq. 4.8 and also  $F_{Longitudinal}$  force was calculated as 21600 N using Eq. 4.9.  $FC_1, FC_2, FC_3, FC_4, FC_5, FC_6, FC_7, FC_8, FC_9, FC_{10}, FC_{11}$  and  $FC_{12}$  are all fully fixed constraints.



(a)



(b)

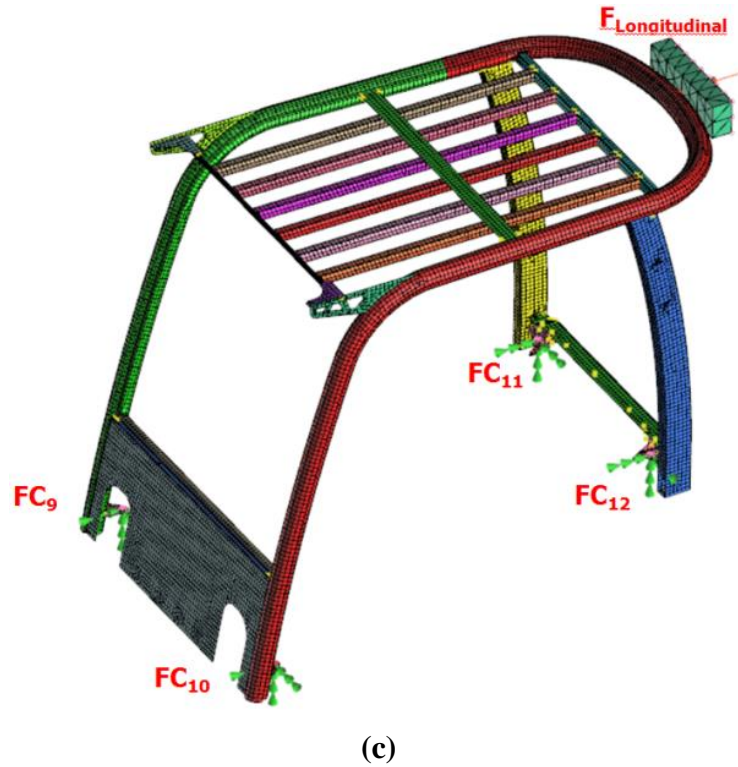
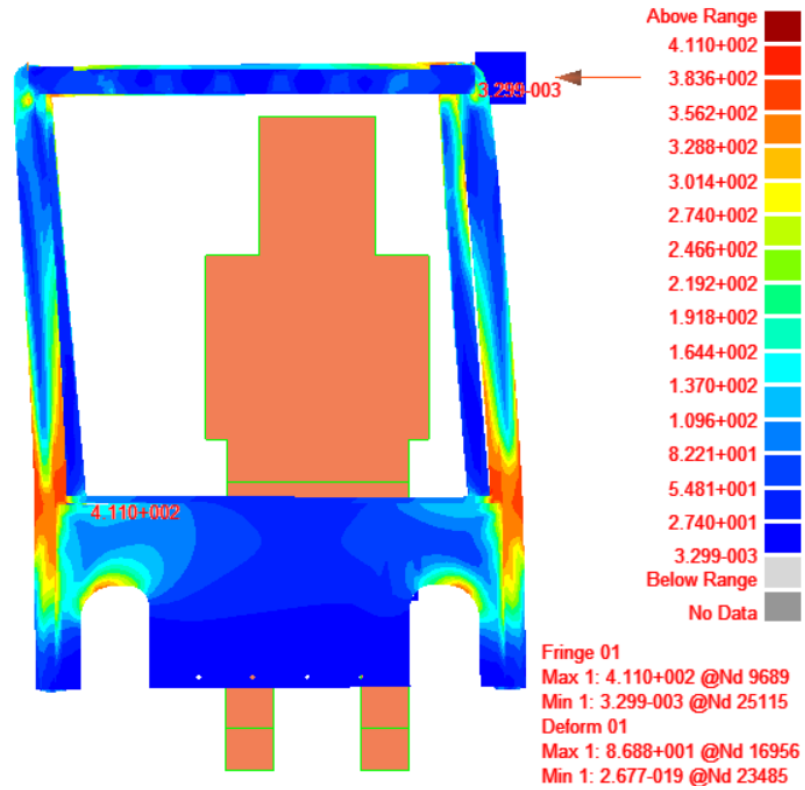


**Figure 4.14.** Loading cases of head-guard. (a)  $F_{Lateral}$  force,  $FC_1$ ,  $FC_2$ ,  $FC_3$  and  $FC_4$  fixed constraints; (b)  $F_{Vertical}$  force,  $FC_5$ ,  $FC_6$ ,  $FC_7$  and  $FC_8$  fixed constraints; (c)  $F_{Longitudinal}$  force,  $FC_9$ ,  $FC_{10}$ ,  $FC_{11}$  and  $FC_{12}$  fixed constraints.

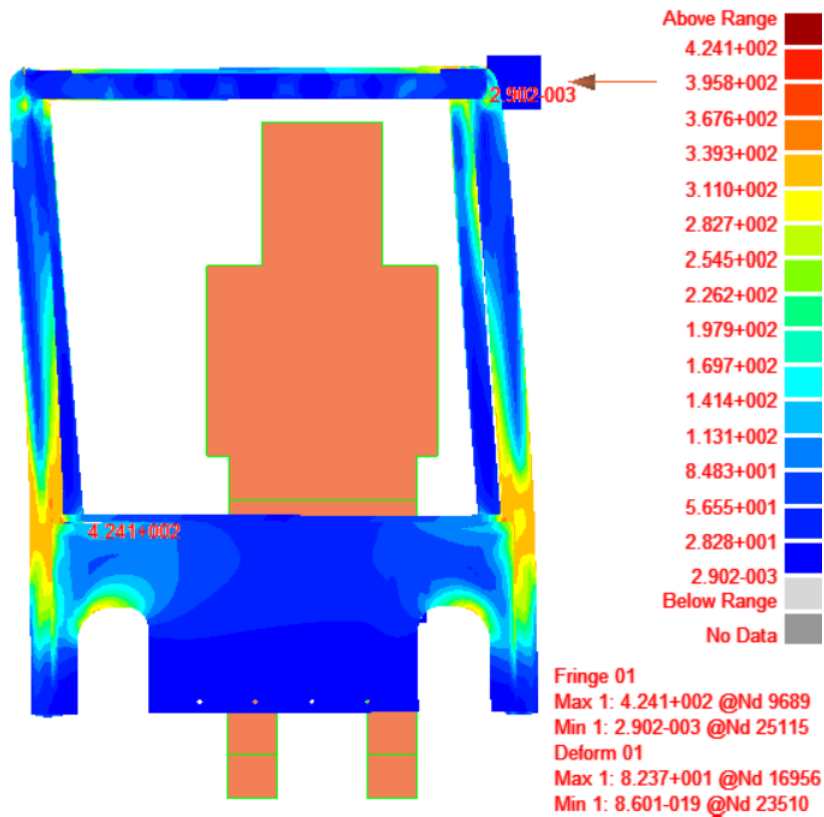
#### 4.4.5 FEM Results of Head-guard

##### 4.4.5.1 FEM Results of Lateral Loading

27000 N lateral loading was carried out using the load distribution device. At the end of the lateral loading, maximum stress value was measured as 411 MPa. Maximum deformation at force applied point was measured as 71.64 mm. FEM results of 27000 N lateral loading is shown on the Fig. 4.15. Force-displacement curve of head-guard at 27000 N lateral loading is given in the Fig. 4.16.



(a)



(b)

**Figure 4.15.** FEM results of 27000N lateral loading (a)Maximum loading; (b)Load removed.

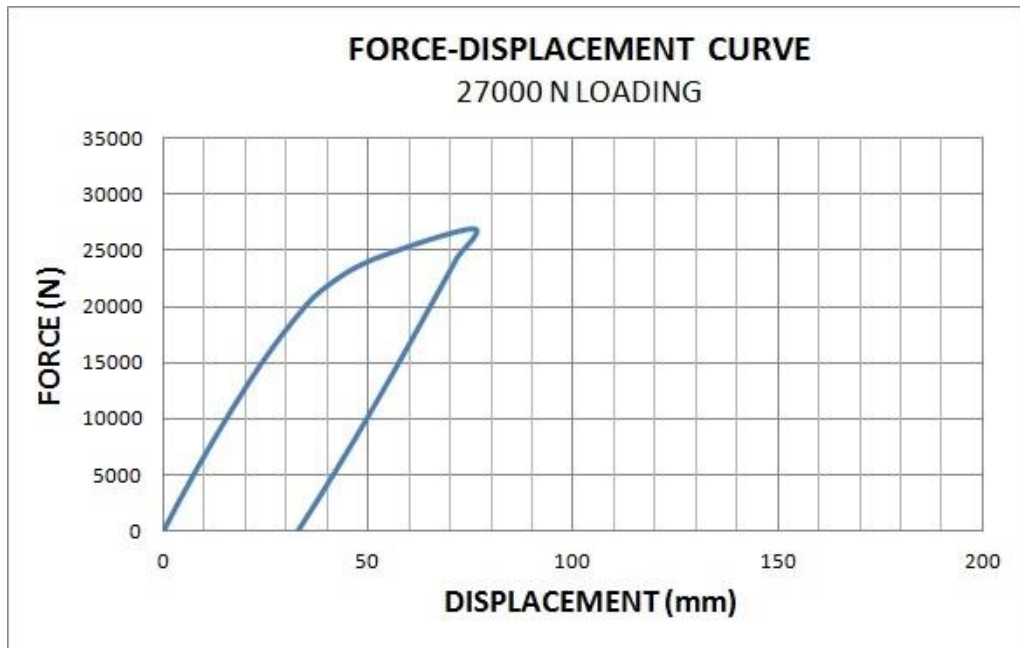
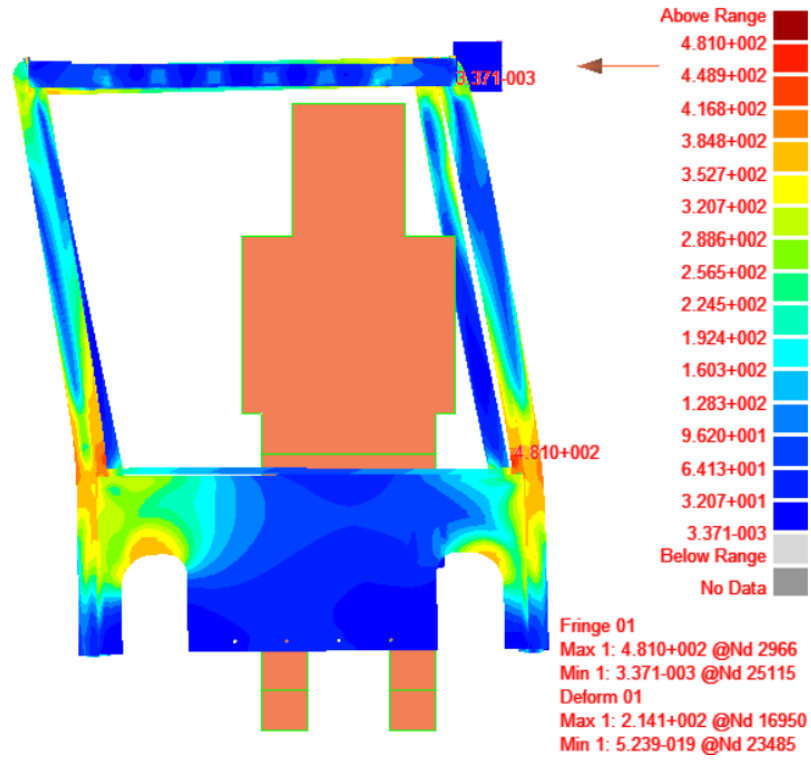


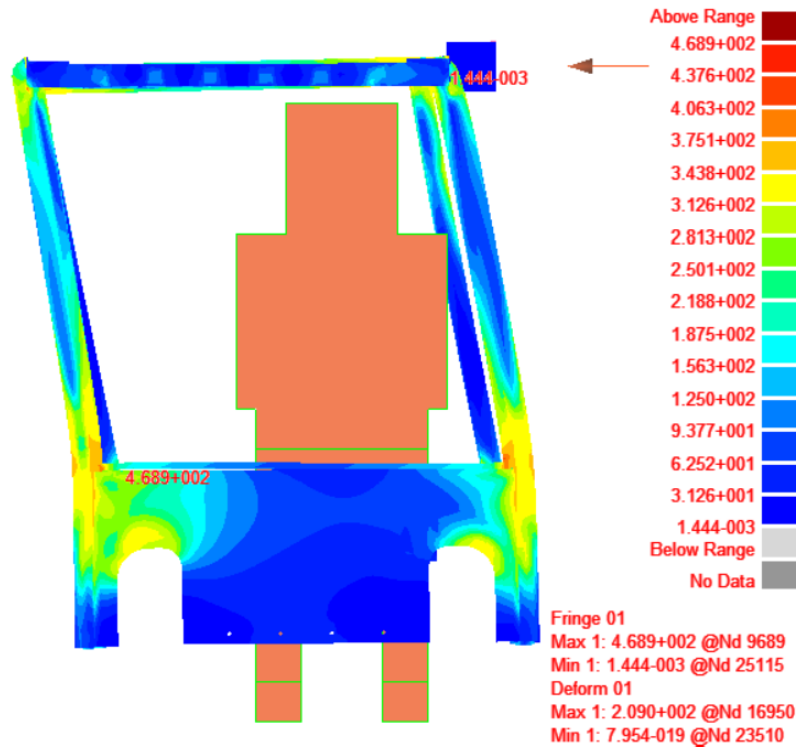
**Figure 4.16.** Force-Displacement curve, 27000N loading.

During the loading, head-guard didn't enter to the area of the seated operator. However, the stress levels on some positions of head-guard were higher than the yield stress values. As a result of this, permanent deformation was observed on head-guard. There were no stress values greater than the ultimate stress. During the lateral loading with a magnitude of 27000 N, energy requirement that specified in the ROPS standard was not met. Specific lateral load energy at 27000 N was calculated as 1373 J and 4607 J energy could not be reached. Because of that, the lateral force was increased until the required energy level is attained.

In the second phase, 32000 N lateral loading is applied. At the end of the lateral loading, maximum stress value was measured as 481 MPa. Deformation at force applied point was measured as 189.5 mm. FEM results of 32000 N lateral loading was shown on the Fig. 4.17. Force-displacement curve of head-guard at 32000 N lateral loading is given in the Fig. 4.18.



(a)



(b)

**Figure 4.17.** The stress results of FEA for the lateral loading with a magnitude of 32000 N (a) When the maximum load is acted; (b) When the load is removed.

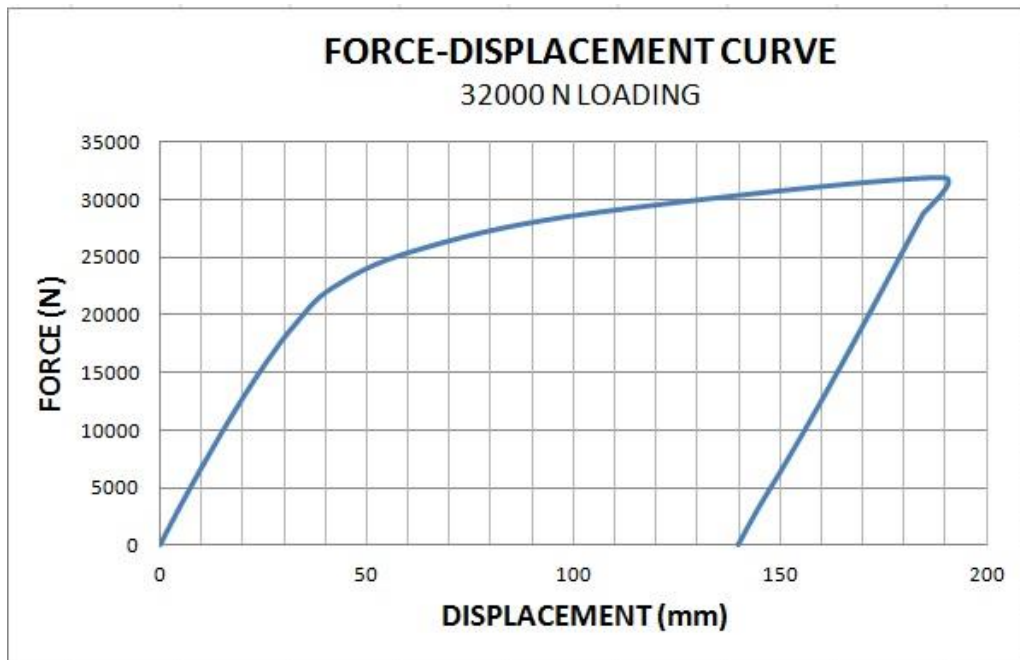
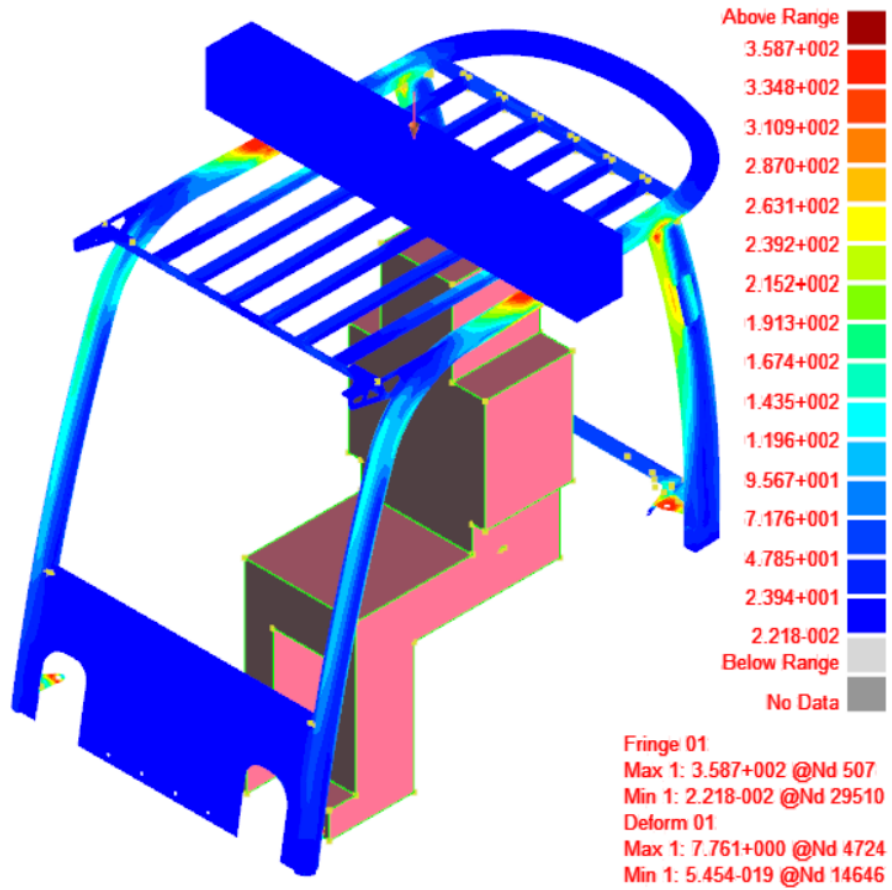


**Figure 4.18.** Force-Displacement curve, 32000N loading.

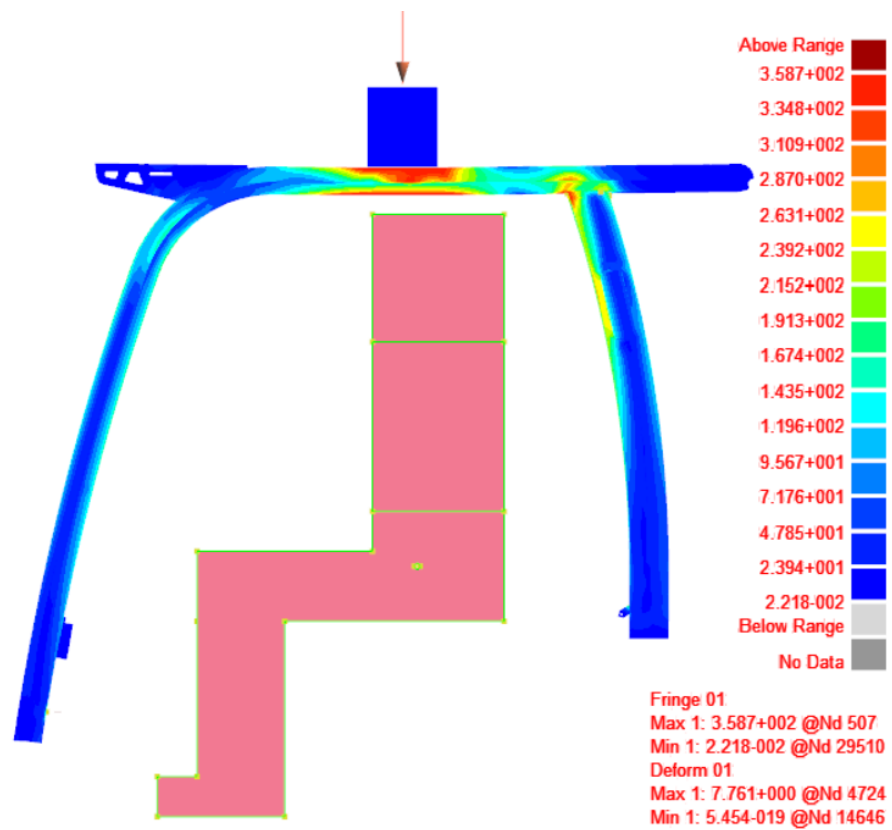
Also during 32000 N lateral loading, head-guard didn't enter to the seated operator area. The stress levels on some positions of head-guard were higher than the yield stress values. As a result of this, permanent deformation was observed on head-guard. All stress values were less than the ultimate stress. The results showed that lateral load with a magnitude of 32000 N satisfies the specified energy requirement in the ROPS standard. Specific lateral load energy under the application of 32000 N load is calculated as 4758 J and so 4607 J energy could be reached.

#### **4.4.5.2 FEM Results of Vertical Loading**

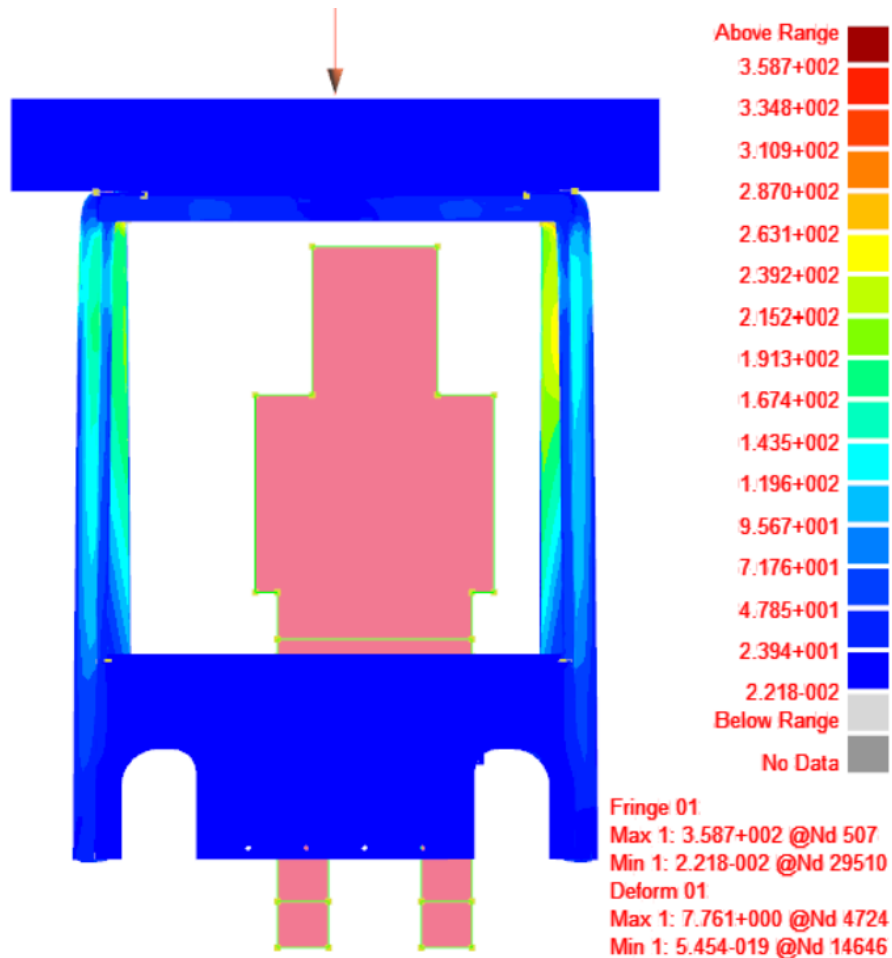
Vertical loading was carried out using the long load distribution device over the cabin. At the end of the vertical loading, maximum stress value was measured as 359 MPa. Deformation at force applied point was measured as 7.8 mm. During the loading, head-guard didn't enter to the area of seated operator. Because stress values near to the load distribution device are higher than the yield stress, head-guard has a permanent deformation. The FEM results of vertical loading was shown on the Fig. 4.19.



(a)



(b)



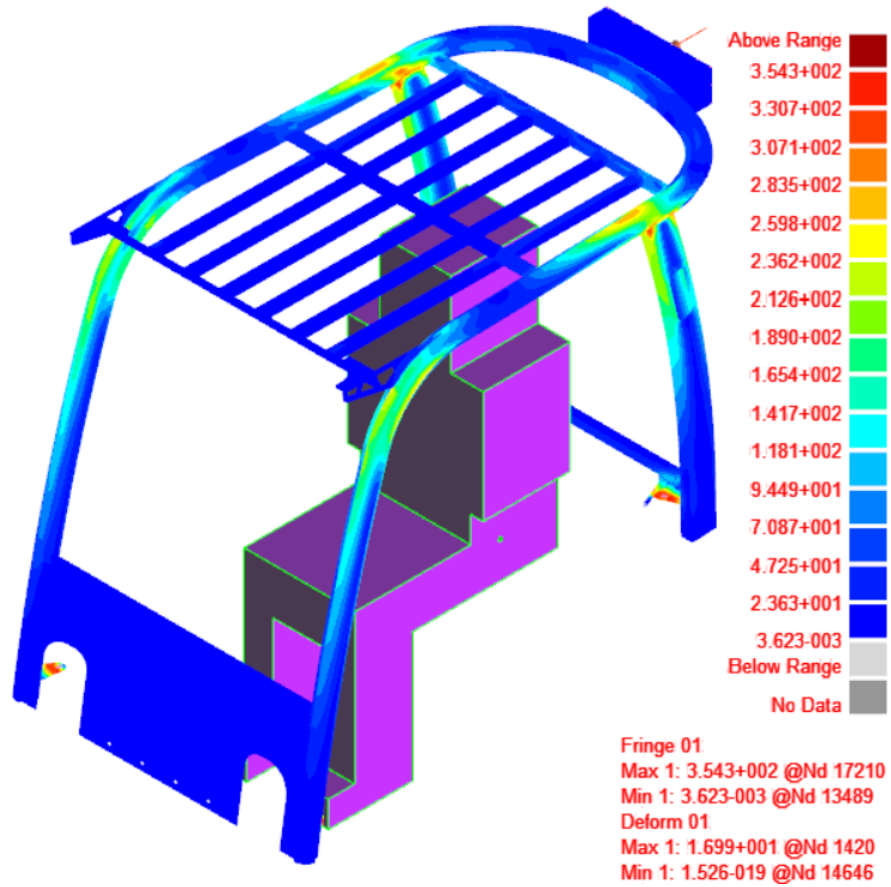
(c)

**Figure 4.19.** The FEM results of vertical loading on (a) Isometric view; (b) Front view; (c) Side view.

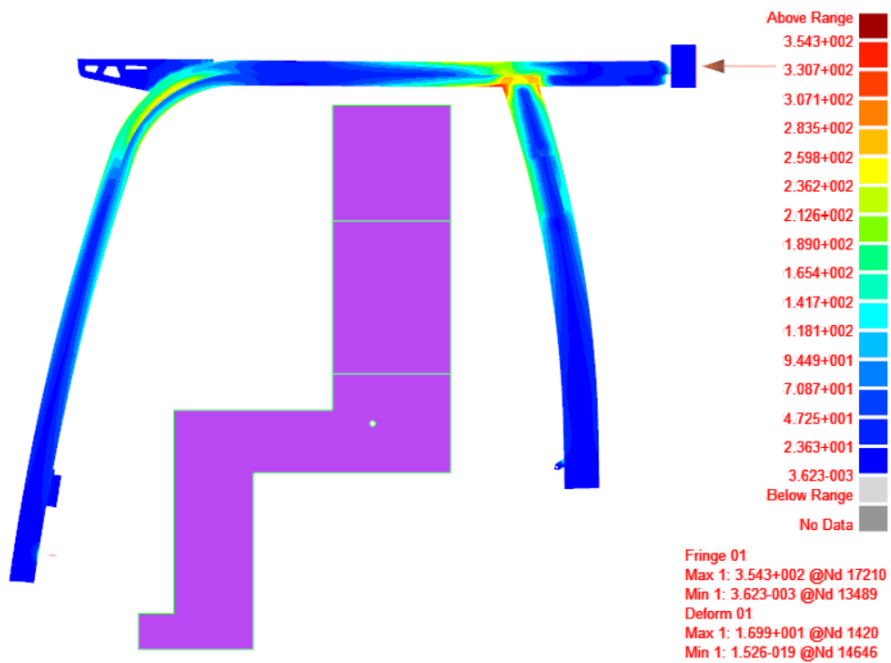
#### 4.4.5.3 FEM Results of Longitudinal Loading

Longitudinal loading was carried out using the load distribution device. At the end of the longitudinal loading, maximum stress value was measured as 354 MPa. Deformation at force applied point was measured as 17 mm. During the loading, head-guard didn't enter to the area of seated operator. Because stress values are below the yield stress, head-guard has no permanent deformation. The FEA results of longitudinal loading was shown on the Fig. 4.20.

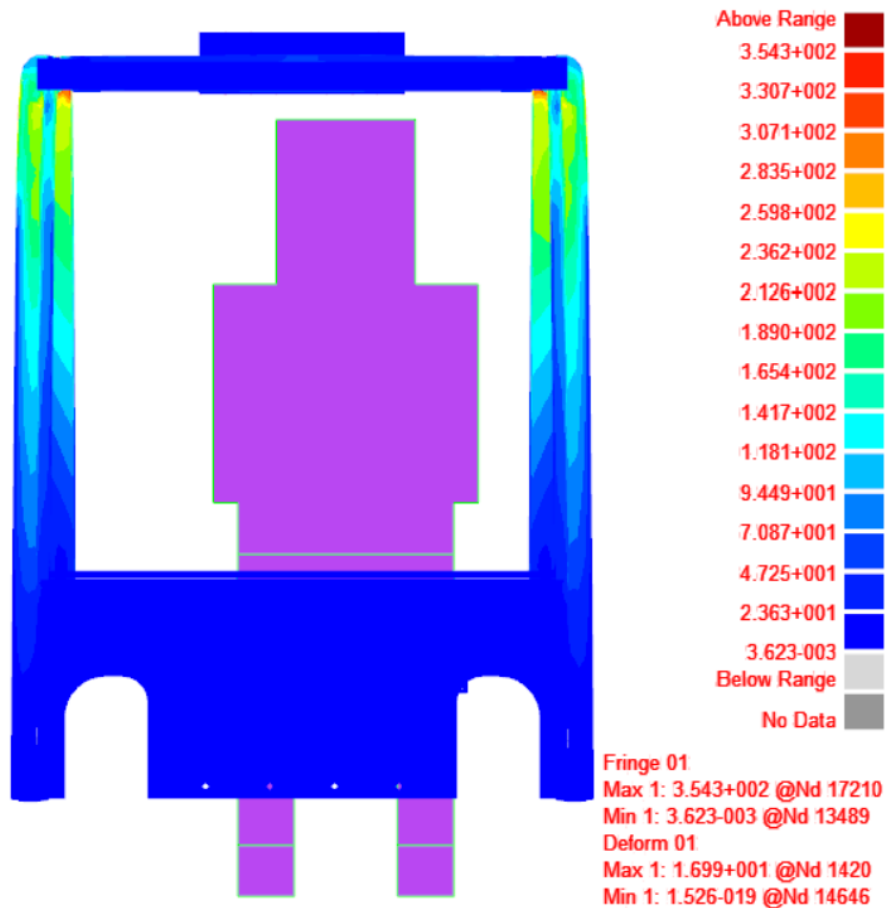




(a)



(b)



(c)

**Figure 4.20.** FEM results of longitudinal loading (a) Isometric view of fem result; (b) Front view of fem result; (c) Side view of fem result.

#### 4.4.6 Conclusion on Finite Element Analysis of Head-guard

In this section, the ROPS analysis of head-guard was performed using finite element method. For all loadings (lateral, vertical and longitudinal), the head-guard didn't enter to the area of seated operator. According to the results of finite element analyses, the head-guard satisfies the requirements of ROPS standard. However, the physical ROPS test have to be performed to verified the results of finite element analyses. Any geometry change wasn't applied to head-guard due to its acceptable performance. However, the reliability of head-guard can be improved by the geometry changes.

## 4.5 Analysis of Fork

Fork, located in front of forklift and mounted to the attachment, is used to carry the loads. The 3D solid model of the fork/forks is shown in Fig. 4.21. The analysis of fork were carried out according to EN ISO 3691 – 1: 2012 Standard [15]. The  $W_1$  load, shown in Fig. 4.4, is applied to the fork at standard load centre distance.  $FC_{13}$ ,  $FC_{14}$ ,  $FC_{15}$  and  $FC_{16}$  are fully fixed constraints that all degrees of freedom is restrained. The various load acting on the fork is shown in Fig. 4.22.

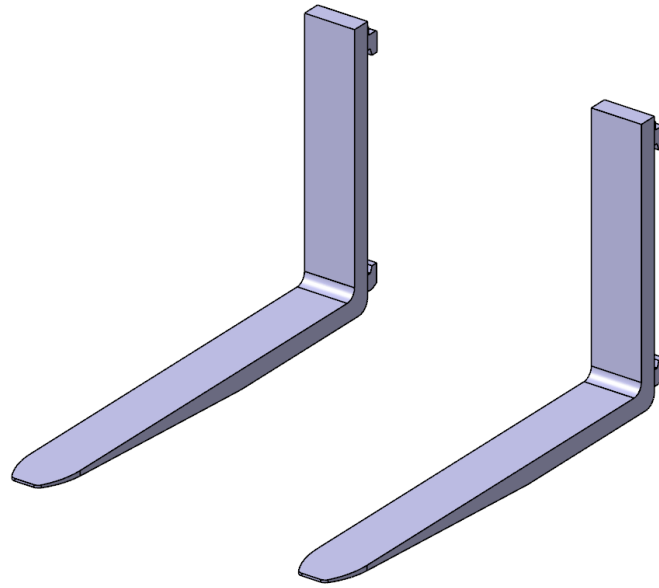


**Figure 4.21.** The solid model of fork.

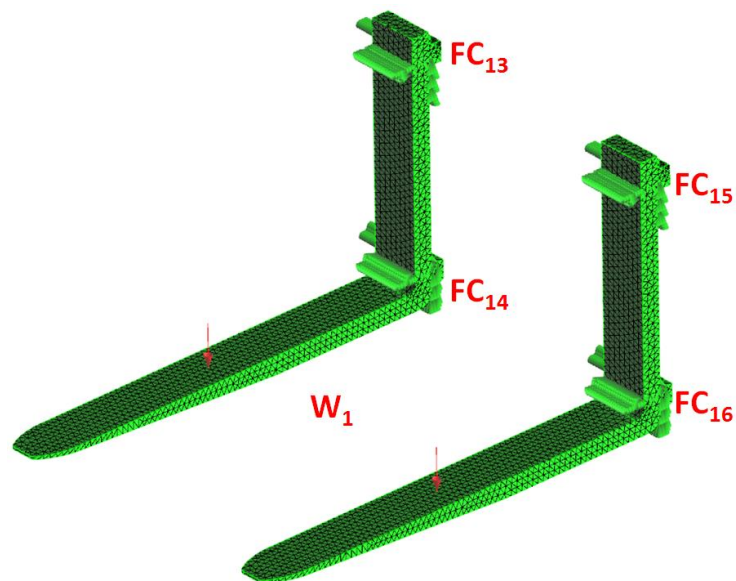


**Figure 4.22.** Finite element model of fork with its boundary conditions.

### 4.5.1 Finite Element Analysis of Fork

In the finite element model of fork, solid mesh is preferred to use due to the structure of the geometry. The solid model of fork, shown in Fig. 4.21, meshed with 35540 solid elements with 58636 nodes in SimXpert Structure Analysis program. The elements type used in the model is CTETRA10. The finite element model of fork is shown in Fig. 4.23. The fork is made of St52-3 and the mechanical properties of St52-3 are given in Table 4.2.

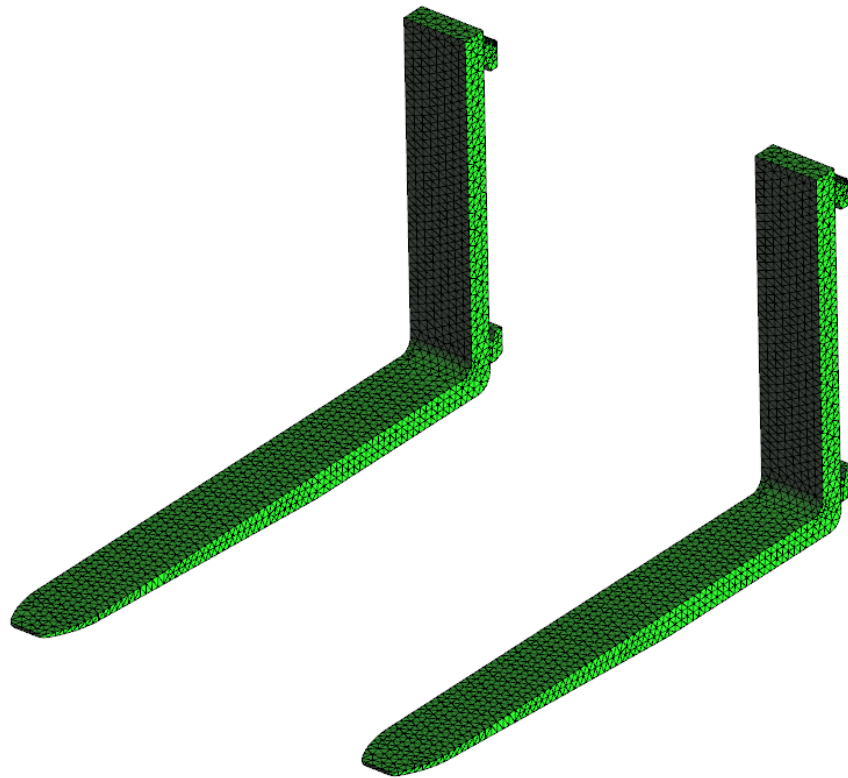
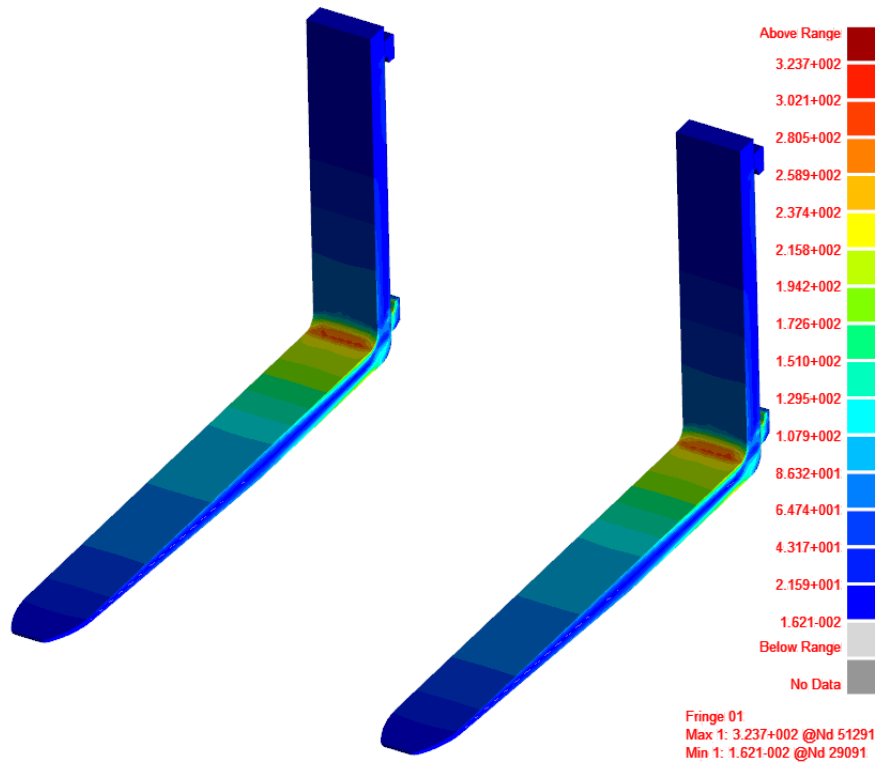


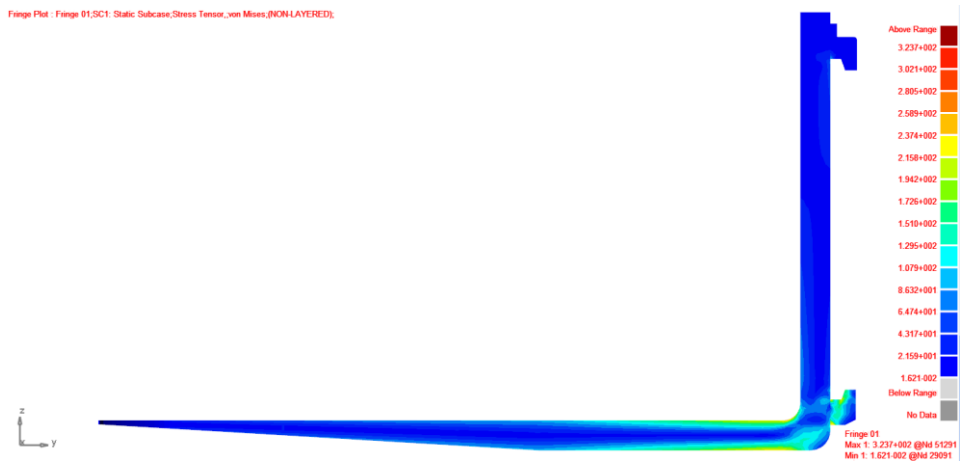
**Figure 4.23.** Finite element model of fork.

### 4.5.2 FEA Results of Fork

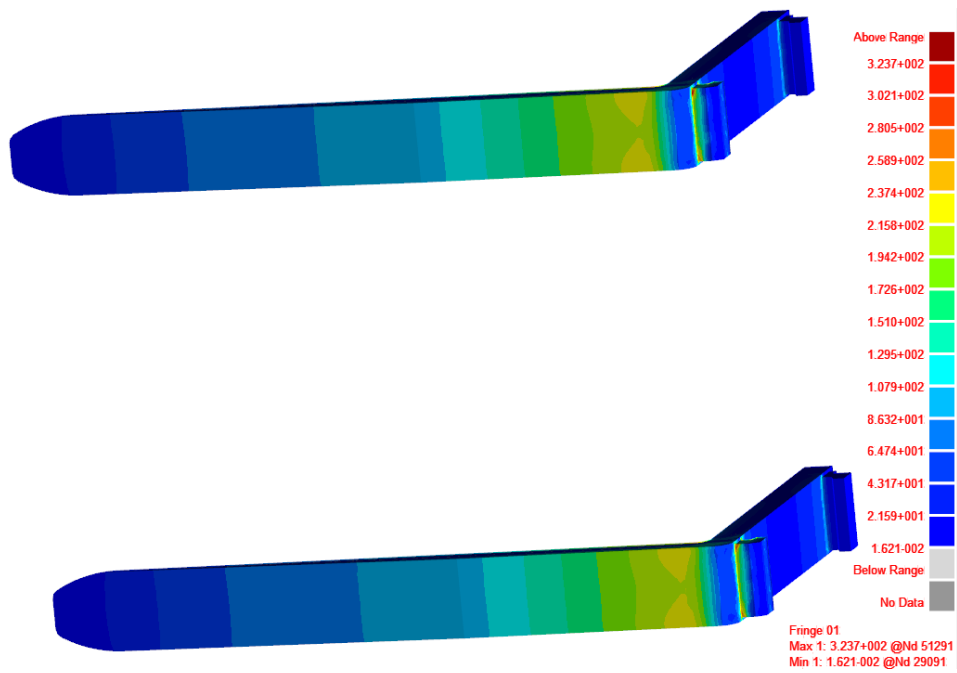
The analysis of fork is carried out in case of overload, and the results are shown in Fig. 4.24. It is shown that the maximum von Mises stress is calculated as 323 MPa and the maximum deformation is calculated as 20.35 mm. Displacement results are shown in Fig. 4.25.



(a)



(b)



(c)

**Figure 4.24.** The FEA results of fork. (a) Isometric view of fork fem result; (b) Side view of fork fem result; (c) Isometric view of fork fem result.

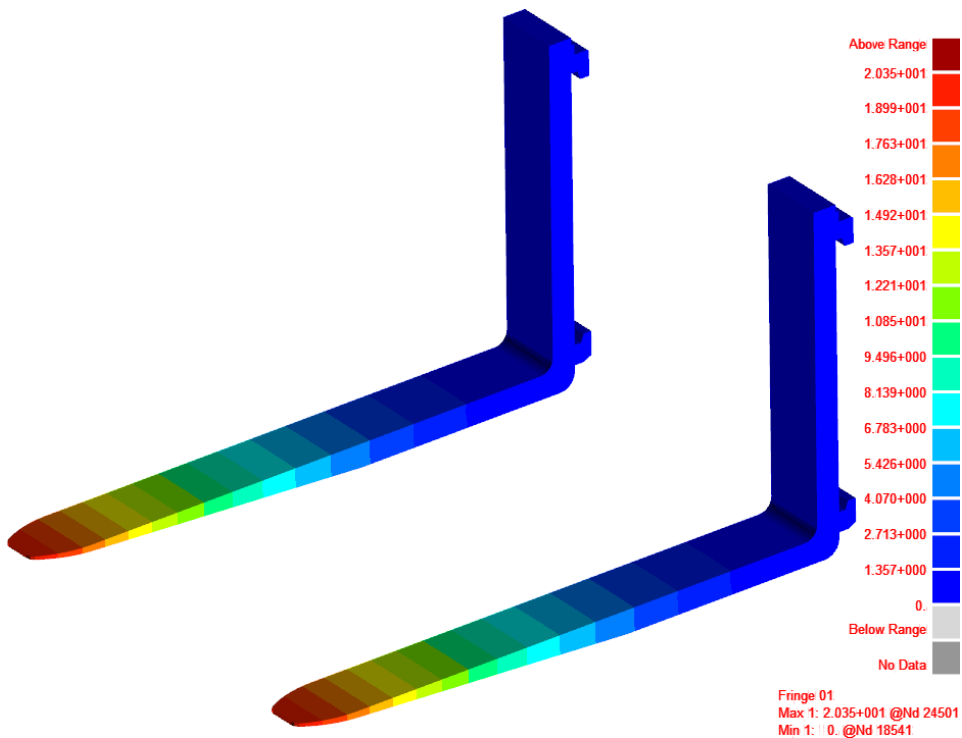


**Figure 4.25.** Displacement result of fork.

### **4.5.3 Conclusion on Finite Element Analysis of Fork**

In this section, the finite element analysis of fork was performed using finite element method. The maximum von Mises stress which was below the yield strength of the fork material was evaluated as 323 MPa. With this result, it can be said that no permanent deformation occurs in the fork. However, the maximum stress value is quite close to yield strength of the material and for the several loading situation it can have some problems. To eliminate this fatigue failure, the geometry of fork or the material selection of fork have to be revised.

## CHAPTER 5

### CONCLUSIONS

In this study, static analyses of structural parts of a diesel forklift truck such as chassis, head-guard and fork have been performed by using finite element method. The possible geometry modifications have been utilized with respect to stress distributions at critical regions in order to reduce stress concentrations and to improve reliability of the forklift design.

Static analysis of chassis was carried out according to EN ISO 3691 – 1:2012 standard [15]. The results of finite element analyses pointed stress concentrations at the connection bracket of tilt cylinders. The geometry of connection bracket was modified to remove or at least to alleviate stress concentrations. The results of finite element analyses of chassis for original geometry and the modified geometries were compared with each other. The results show that the modified geometries have lower stresses than original geometry. It is also seen that the factor of safety is increased to 2.08 from 1.38. According to the results, it can be said that the reliability of connection bracket of tilt cylinder and so that the chassis have been improved. The reliability can also be further enhanced by additional geometry changes.

The ROPS analysis of head-guard is performed using the finite element method. The maximum stress and the deformation values have been evaluated by considering the lateral, vertical and longitudinal loading situations of ROPS. The deformation results under these loadings show that head-guard can have permanent deformation. However, their levels are far away from the risk of any injury of the seated operator. According to the results of finite element analyses, the head-guard satisfies the requirements of ROPS standard and there is no need to make geometry modification about head-guard. However, the experimental procedure of ROPS analysis must also be performed to verify the results of current finite element analyses.

The finite element analysis of fork was also performed by considering the overloading situation and the application of load at standard load distance. The



results of finite element analysis show that the maximum von Mises stress is below the yield strength of the fork material. Due to that, no permanent deformation occurs in the fork. However, the maximum value of evaluated stress is 323 MPa and it is quite close to yield strength of the material. It can have some problems for the several loading. The geometry of fork or the material selection of fork have to be revised to eliminate possible problems.

## **FUTURE WORKS**

In this work, finite element analyses of chassis, head-guard and fork of forklift were performed under static load applications. The dynamic analysis of these structures can also be performed to obtain more accurate results by simulating real situations.

The optimization techniques such as topology optimization can be carried out on chassis to reduce material cost and weight without decreasing the reliability of chases.

To improve design reliabilities of head-guard and fork, geometrical improvements can be provided.

Furthermore, the mast assembly and rear axle can also be analyzed and the FOPS analyses of head-guard can be carried out to improve the reliability.

## REFERENCES

- [1] Bhagat, V. K., Wankhade, P. A., Gosh, P. P. (2012). Development and structural analysis of translation carriage for reach truck, *International Journal of Applied Research in Mechanical Engineering*, **2(2)**, 93-99.
- [2] Doçi, I., Imeri, V. (2013). Dynamic analysis of forklift during load lifting using modelling and simulations, *International Journal of Current Engineering and Technology*, **3(2)**, 342-347.
- [3] Meshram, A. T. (2013). Finite element mast assembly of material handling equipment, *International Journal of Technology*, **3(1)**, 50-55.
- [4] Rane S. B., Shirodkar, H., Reddy, P. S. (2013). Finite element analysis and optimization of a forklift chassis, *Altair Technology Conference*, **1**, 1-6.
- [5] Cline K. (2004). Failure of a High-Capacity Forklift Fork, *Microscopy Society of America*, **10.S02**, 776-777.
- [6] Miralbes, R., Malon, H., Castejon, L. (2011). Design of Accesories fort he Coupling in Forklift Trucks: Crane Gibs and Pallet Box Lock, *Selected Proceedings from the 15th International Congress On Project Engineering*, 233-246.
- [7] Stoychev, G., Chankov, E. (2009). Investigation of Dynamic Stresses In a Forklift Truck Lifting Installation, 75-80.
- [8] Todorov, G., Ivanov, M., Kamberov, K., Stoev Sv. (2011). Design and Virtual Prototyping of a Forklift Transmission Module, 37-40.
- [9] Slavchev, Y. (2009). 3-D Research on Fork Arms of Forklift Trucks, *Proceedings of the International Conference on Manufacturing Systems*.

- [10] Yao, W., Dingxuan, Z., Lei, W., Lili, W. and Yanjuan, H. (2015). Analysis of New Type Elevating Mechanism for Hybrid Forklift Based on ANSYS, *5th International Conference on Advanced Design and Manufacturing Engineering*.
- [11] Sachin S., U., Aakash G., P., Vishal V., Makarand M., G. and Prashant R., K. (2014). Design and Structural Analysis of Mechanical Forklift using ANSYS Software, *International Journal of Research in Advent Technology*, **2(5)**.
- [12] Zeng, H., Li, T., Gao, Q. and Liu, S. (2009). The CAE Analysis of Fork Truck Frame System Based on ADAMS and ANSYS, *Applied Mechanics and Materials*, **16(19)**, 1149-1153.
- [13] Figueiredo, M. V., Oliveira, F. M. F., Gonçalves, J. P. M., de Castro, P. M .S. T. and Fernandes, A. A. (2001). Fracture analysis of forks of a heavy duty lift truck, *Engineering Failure Analysis*, **8(5)**, 411–421.
- [14] Erkliđ, A., Yeter, E. (2013). The Improvements of the Backhoe-Loader Arms. *Modeling and Numerical Simulation of Material Science*, **3(4)**, 142-148.
- [15] EN ISO 3691 – 1: 2012 Standard. Industrial trucks - Safety requirements and verification - Part 1: Self-propelled industrial trucks, other than driverless trucks, variable-reach trucks and burden-carrier trucks.
- [16] EN ISO 3471: 2008 ROPS standard. Earth-moving machinery - Roll-over protective structures - Laboratory tests and performance requirements.
- [17] Zienkiewicz, O. C., & Taylor, R. L. (2005). The finite element method for solid and structural mechanics. *Butterworth-heinemann*.
- [18] Shen, S. F. (1977). Finite-element methods in fluid mechanics. *Annual Review of Fluid Mechanics*, **9(1)**, 421-445.
- [19] Desmet, W., & Vandepitte, D. (2010). Finite element modeling for acoustics. *Lecture Notes of the ISAAC21 Course*. KU Leuven, Leuven, Belgium, **4**, 22-25.
- [20] Coggon, J. H. (1971). Electromagnetic and electrical modeling by the finite element method. *Geophysics*, **36(1)**, 132-155.

- [21] Schneider, G. E., & Raw, M. J. (1987). Control volume finite-element method for heat transfer and fluid flow using collocated variables—1. Computational procedure. *Numerical Heat Transfer, Part A Applications*, **11(4)**, 363-390.
- [22] Hrennikoff, A. (1941). Solution of problems of elasticity by the framework method. *Journal of applied mechanics*, **8(4)**, 169-175.
- [23] Clough, R. W. (1960). The finite element method in plane stress analysis.